



The Abdus Salam
International Centre for Theoretical Physics



2168-16

**Joint ICTP-IAEA Workshop on Dense Magnetized Plasma and Plasma
Diagnostics**

15 - 26 November 2010

Plasma-Focus PF-3

V. Krauz
*Kurchatov Institute
Moscow
Russian Federation*

Plasma-Focus PF-3

V.I.Krauz
and PF-3 team
RRC “Kurchatov Institute”
Moscow, Russia

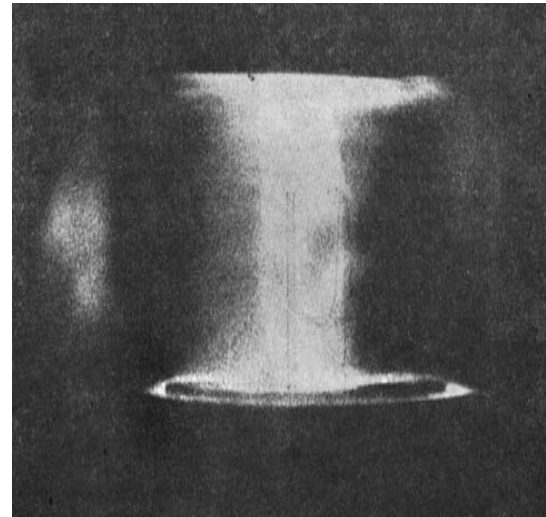
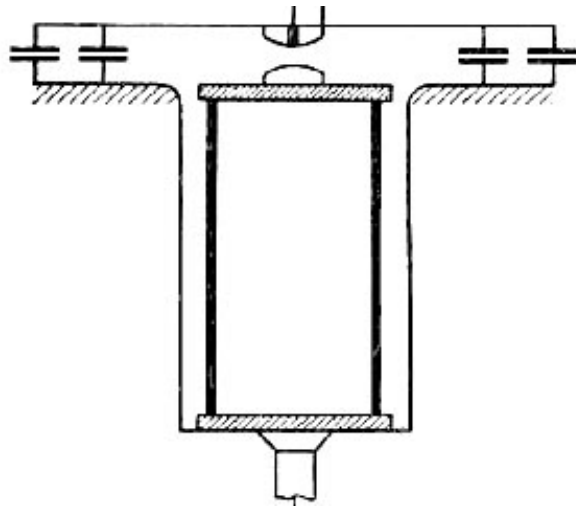
**Joint ICTP-IAEA Workshop on Dense Magnetized Plasma
and Plasma Diagnostics, 15 to 26 November 2010**

Outline

- **History**
- **Filippov-type PF – main features**
- **Plasma Focus PF-3: design and parameters**
- **PF-3 as a source of SXR**
- **PCS dynamics**
- **New approaches in PF studies:**
 - **Astrophysics simulation**
 - **Experiments with liners**
 - **Experiments with dust**
 - **Nanoparticles and nanofilms production**
- **Summary**



***Intensive studies of Z-pinchs were started at
Kurchatov Institute in 1952***



$$I = 500 \text{ kA}, \quad V = 50 \text{ kV}, \quad C = 82 \text{ } \mu\text{F}, \quad t = 10 \text{ } \mu\text{s},$$
$$Y_{\text{DD}} = 10^8$$

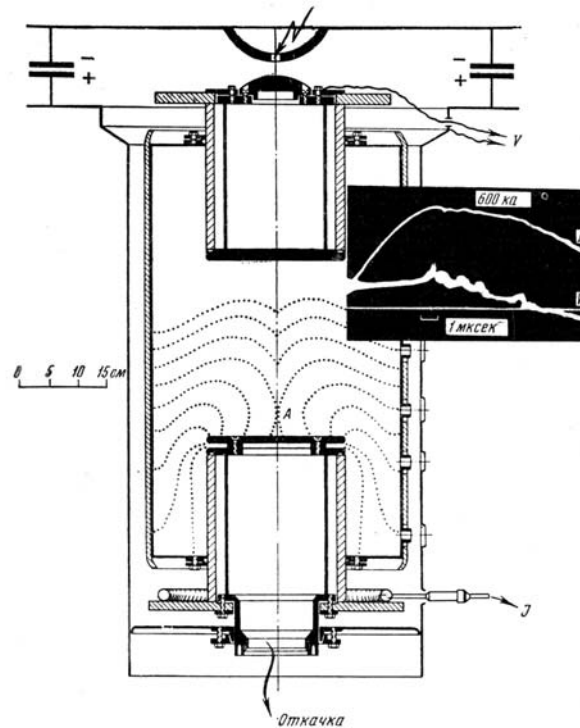
The young scientist N.Filippov was one of the active participants of these experiments in which the fusion neutrons have been discovered.

Z-pinch in the chamber with conducting walls

*D.Petrov, N.Filippov, T.Filippova, V.Khrabrov,
(Plasma Phys. Probl. Contr. Thermonuclear. Reactions , v.4, 1958)*

In this design the insulator "is hidden" and is not in direct visibility of the pinch, that allows to decrease essentially a flux of the radiation from the plasma on the insulator surface and, accordingly, impurity admission.

$C=85-145 \mu\text{F}$,
 $V=15-45 \text{ kV}$,
 $P=0.02-60 \text{ Torr}$,
 $I_{\text{max}} = 100-600 \text{ kA}$



Neutron radiation collimation technique and magnetic probes measurements:

- *the discharge take place along the anode insulator*
- *the neutron source is near the anode surface*

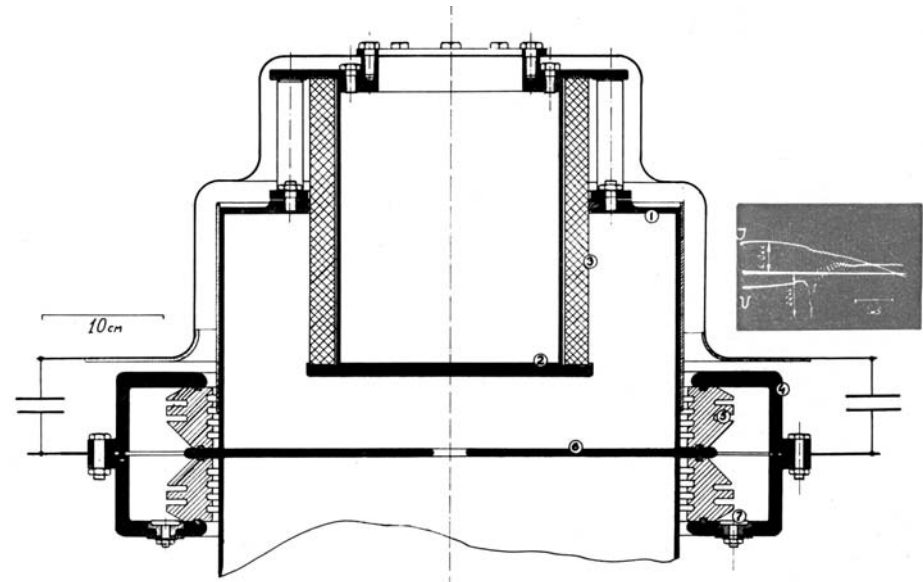
Neutron yield of $5 \cdot 10^9$ was achieved!

Noncylindrical Z-pinch

*N.Filippov, T.Filippova, V.Vinogradov,
Salzburg 1962 (Nucl.Fusion, Suppl., Pt.2, 1962)*

Plasma focus basic properties and main parameters were established

Average plasma density	10^{19} cm^{-3}
Plasma temperature	0.8-1.2 keV
Diameter of compression zone	5 mm
Diameter of hot zone	1-1.5 mm
Volume of hot plasma	$3 \cdot 10^{-2} \text{ cm}^{-3}$
Time of life	$\sim 200 \text{ ns}$
Implosion velocity	$(2-3) \cdot 10^7 \text{ cm/s}$



Due to high intensity of fusion reactions and small size of fusion source the proton spectrum was measured and SXR image was obtain for the first time

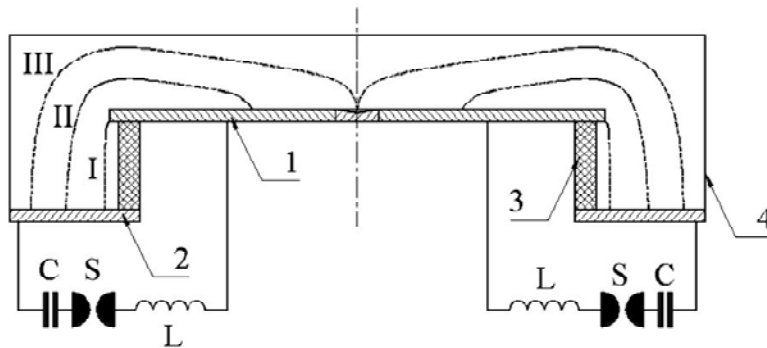
Plasma Focus

The first landmark: Plasma Focus Filippov's type

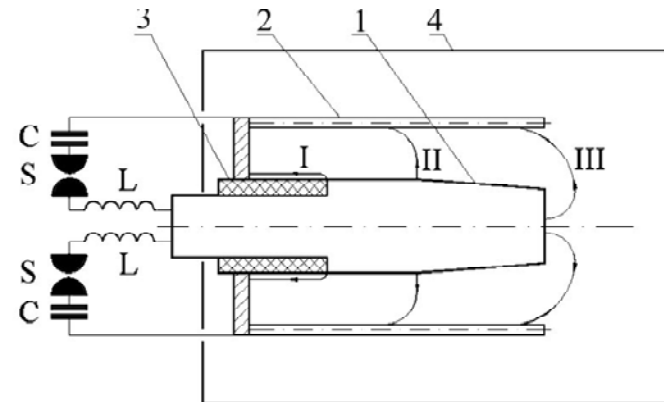
The second landmark: Discovery of the similar phenomenon in Marshall guns
 J.W.Mather: Bull. Am. Phys. Sos., 1964, V.9; Phys. Fluids, 1965, V.8

These two events became an incitement to a new surge of interest in Z-pinch researches over all the world during several consequent decades

Filippov-type ($D/L \gg 1$)



Mather-type ($D/L < 1$)

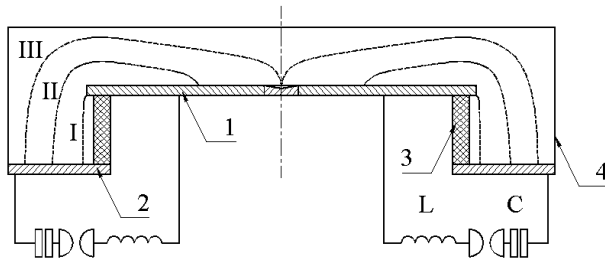


1 – anode, 2 – cathode, 3 – insulator, 4 – vacuum chamber, C – power supply, L – external inductance, S – spark gap. I – break-down phase; II – run-down phase; III – dense plasma focus phase

Despite obvious distinctions in the design and in a direction of researches, final plasma parameters have appeared marvelously similar.

Filippov-type PF – main features

Distinction in the geometry of electrode system first of all affects development of initial, "preparatory" stages of the discharge.



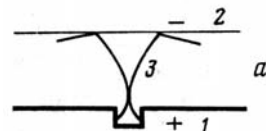
The important difference of the process of the PCS movement in the Filippov-type discharge is that dynamics of PCS is not regulated by the discharge system geometry.

PCS, along with compression to the axis, makes complex movement upwards and sideways.

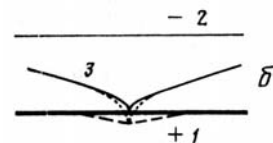
The change of the inductance in time has more complex character.

Very important property of the PF-discharge is non cylindrical shape of the PCS.

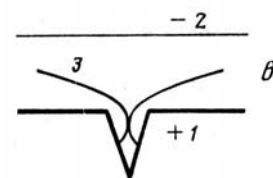
Neutron mode



X-Ray mode



Ion mode



Due to long stage of the radial compression in FPF one can change the degree of the PCS non cylindricity. It is possible, by changing the anode shape, to affect essentially the discharge mode and to optimize the discharge respective various radiations.

N.V.Filippov Sov. J. Plasma Phys. 9 (1), 1983

Surface effects

The Filippov-Type PF is especially an electrode system.

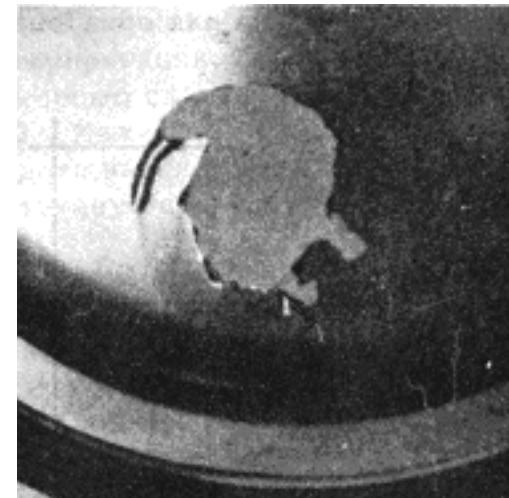
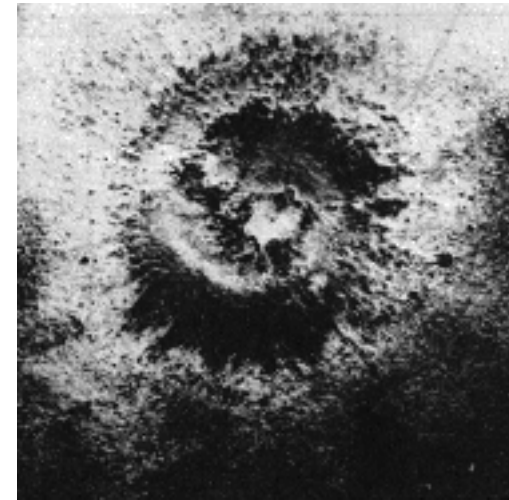
Processes on plasma-anode surface border become priority in the mechanisms of the radiation generation, in particular, in generation of electron and ion beams, HXR.

The mode with PCS “run-away” in which current compression is not accompanied practically by plasma compression was found out.

V.A.Agafonov et al, 3rd Int. Conf. on PP and CNF Res. Novosibirsk, 1968, IAEA, Vienna, 1969.-V.2.-.21-37.

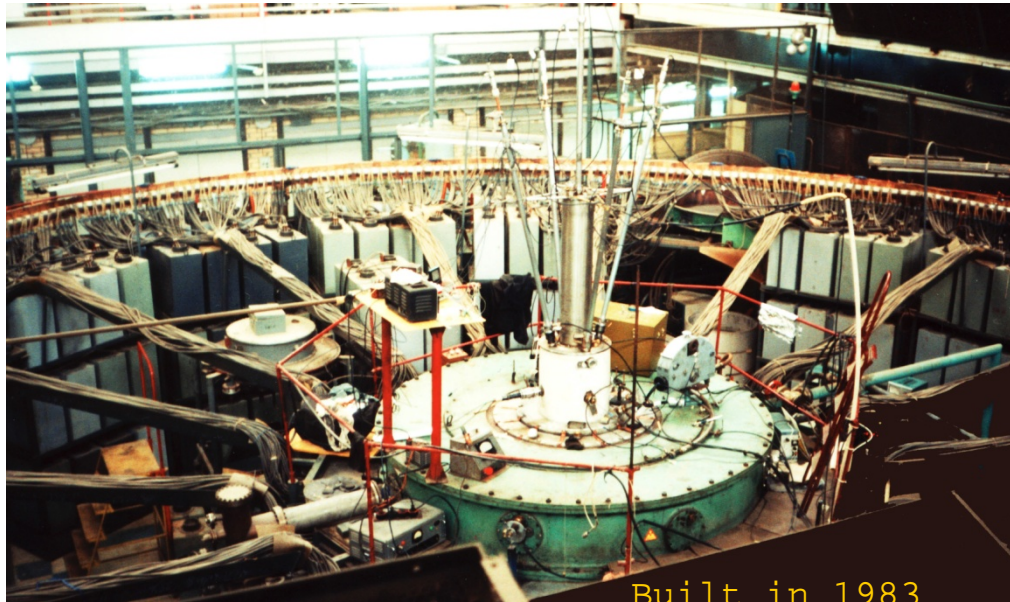
N.V.Filippov, et al., Plasma Phys. and Contr. Nucl. Fus. Res., IAEA, Vienna, 1975, v.III, p.133

This effect essentially affects the PCS dynamics, especially at operation with heavy highly radiated gases.



Photos of an internal and external surface of the flat thin anode in the “run-away” mode 8

Plasma Focus PF-3



FIELDS OF ACTIVITY

- ✓ Dynamics of plasma focus discharge in heavy gases at high level of power input
- ✓ X- ray radiation of high-current neon pinch and its interaction with matter
- ✓ Axial plasma jet studies, Experimental simulation of collisionless shock waves
- ✓ Usage PF as a driver for magnetic compression of liners
- ✓ Experiments with dust plasma
- ✓ New approaches to nanofilms production

The diameter of the anode and that of the chamber equal 1 m and 2,5 m, respectively

The height of an insulator is 26 cm

The distance between anode and upper cover of discharge chamber (cathode) is 22 cm

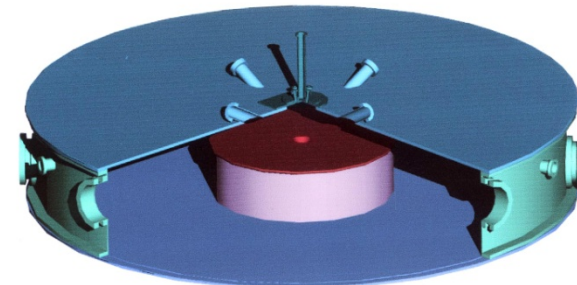
Maximal energy stored at the power supply ($C_{\max}=9,2$ mF, $V_{\max}=25$ kV) is 2,8 MJ

Short-circuit current is 19 MA

Operating energy up to 1 MJ

Discharge current on the plasma load up to 4 MA

Working gas are neon, argon or deuterium at a pressure of 1--10 Torr



Diagnostics

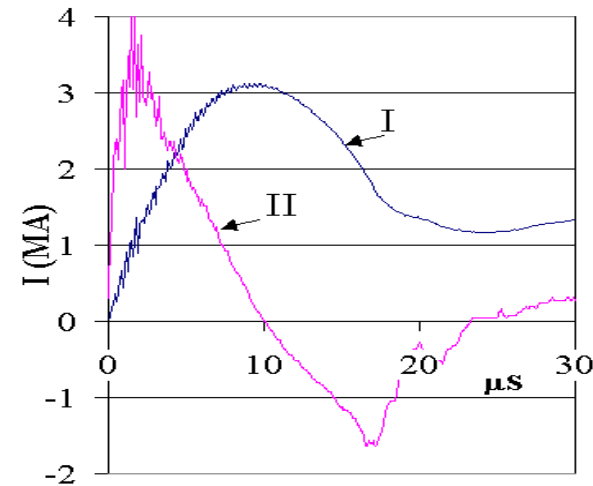
- ✓ Measurement of a discharge current and that of its derivative with the Rogowski coil and with the magnetic coils;
- ✓ Pin-hole cameras: on the side chamber wall at the angle 90° to the system axis and on the upper flange at the angle of 60° .
- ✓ Pin-diodes for measuring the X-ray radiation in the range $0.1 \div 100$ keV with the time resolution $1.5 \div 3$ ns.
- ✓ PM with plastic scintillator for neutron and X-ray measurements in time.
- ✓ Magnetic probes of a special design for studies PCS dynamics and structure.
- ✓ 4 frame cameras at the frame exposure of 12 ns and with time delay between frames of $150 \div 200$ ns.
- ✓ Neutron activation detectors (Ag and In).
- ✓ De Broigle - type and Johann - type spectrometers.
- ✓ Optical spectroscopy.
- ✓ Single-pass Makh-Rozdestvensky interferometer with the arm of 4.8 m and with the aperture of 10 cm

Current limitation

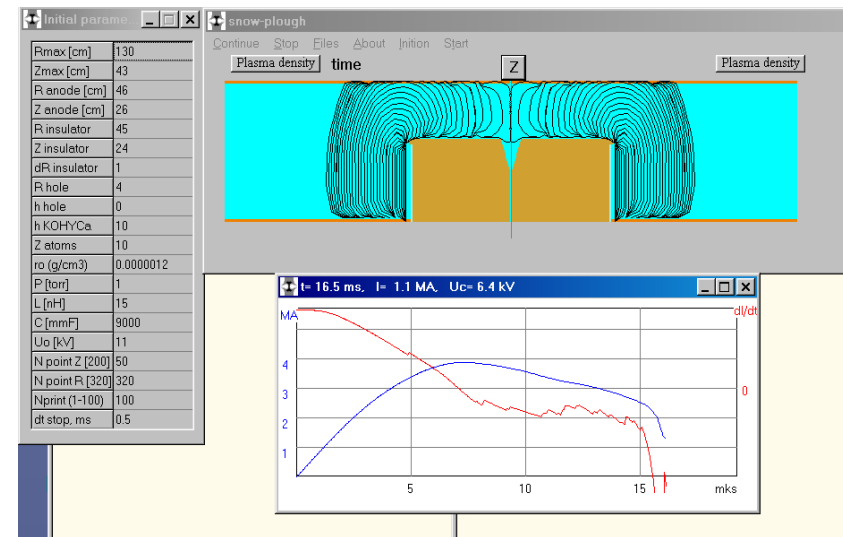
An analysis of the current oscillograms at PF-3-facility has shown that the achievement of high current magnitudes is preventing by the inductive drop related with the current sheath dynamics.

One of the main reasons resulting in an early current “decay” is a practically unlimited PCS-expansion that results in an undesirable increase in the discharge loop inductance.

The current drops almost to half its maximal value at the instant of the maximal compression to the axis.



W=640 kJ, P=4 Torr Neon

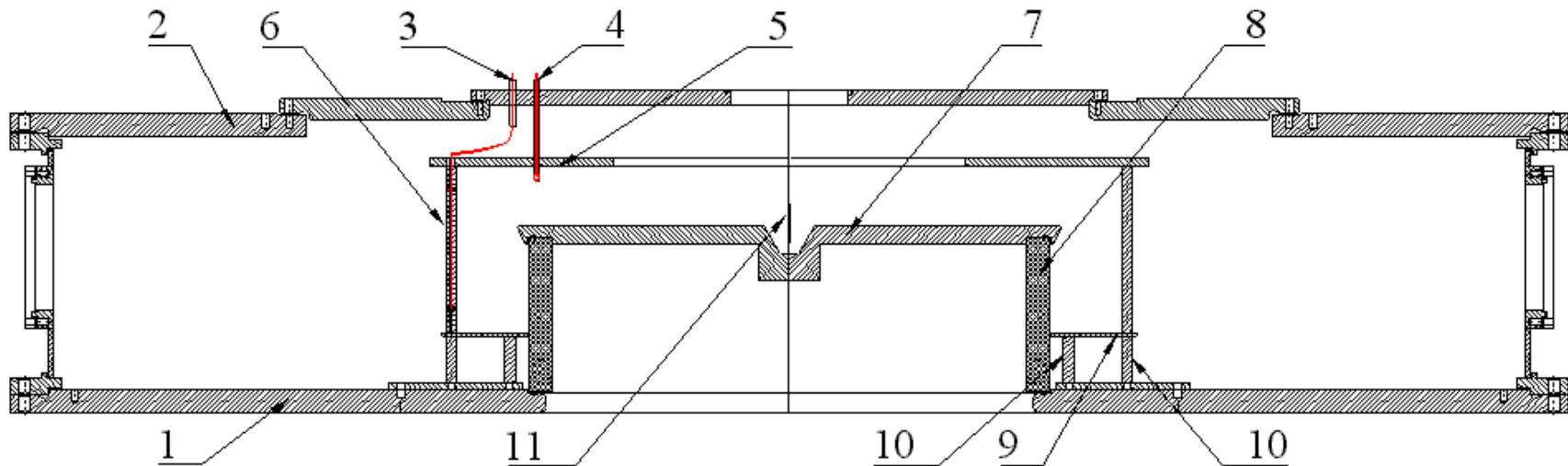


Design of Modernized Discharge Chamber

M.A.Karakin et al., BEAMS'04, p. 738-741

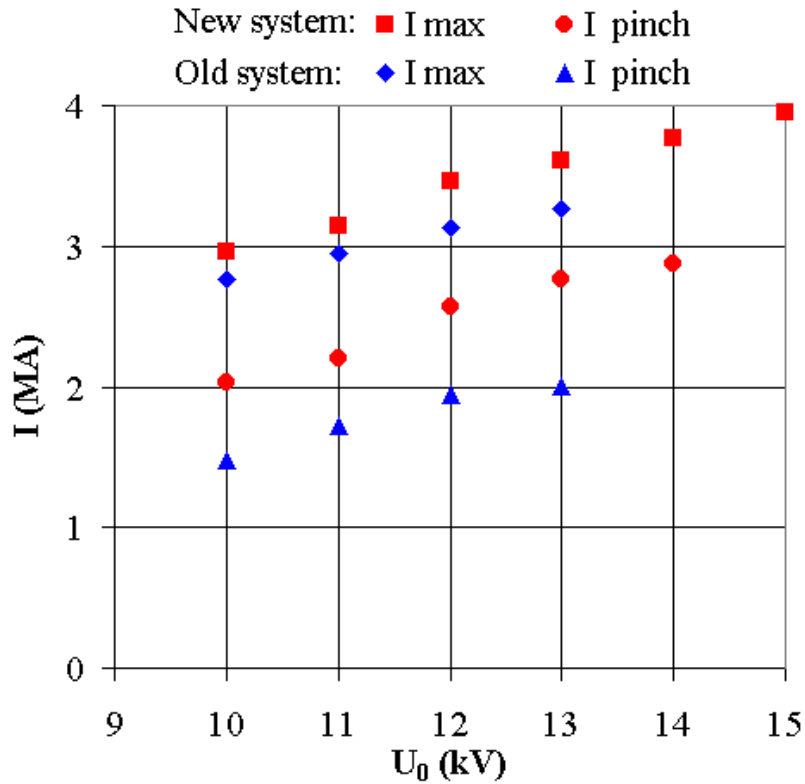
48 rods were installed at the diameter of 115 cm as a “squirrel cage”, playing the role of a sidewall for the reverse current conductor.

Electrode gap between the anode and the chamber upper cover and the working height of the insulator have been also reduced.



1 – chamber floor (cathode); 2 – chamber upper cover; 3 – Rogowski coils; 4 – magnetic probe; 5 – upper flange of reverse current conductor (RCC); 6 – RCC rods; 7 – anode; 8 – insulator; 9 – false-cathode; 10 – false-cathode support rods; 11 – pinch.

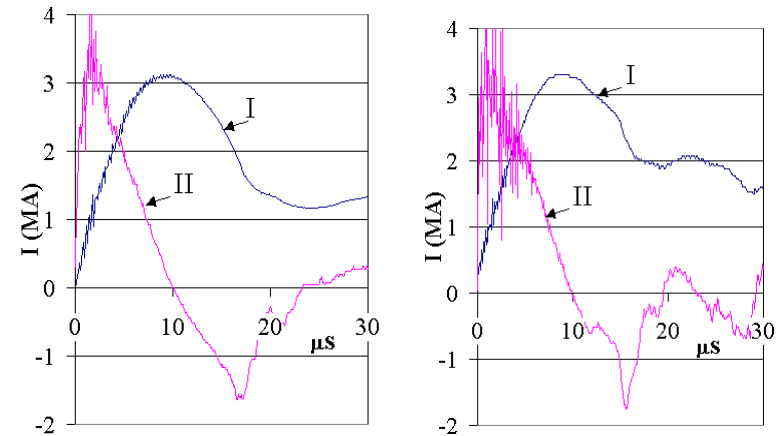
Current Dependence on Voltage



$L_0=15$ nH, $P=4$ Torr

*DISCHARGE CURRENT (I)
and
CURRENT DERIVATIVE (II)*

$W=640$ kJ, $P=4$ Torr Neon



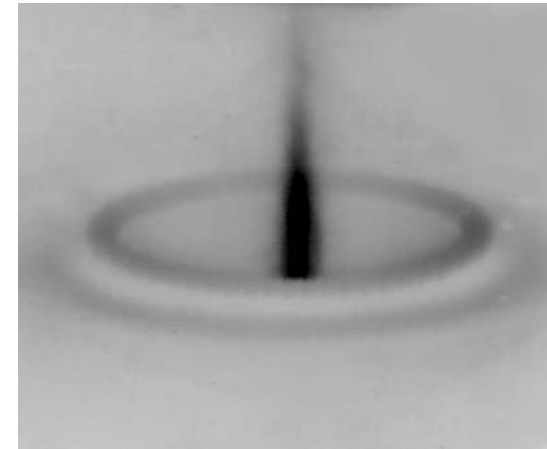
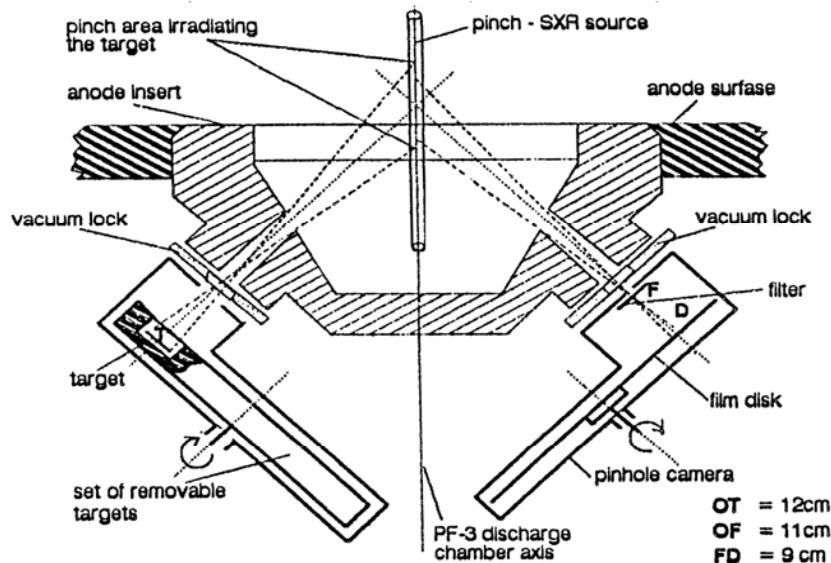
non modernized
discharge systems

modernized
discharge systems

The most part of the results presented below
has been obtained in the modernized system

*PF-3 facility as a source of
soft X-ray radiation*

SXR-yield measurements



10 cm

A number of experiments on PF optimization as a source of a soft X-ray radiation was done in the eighties

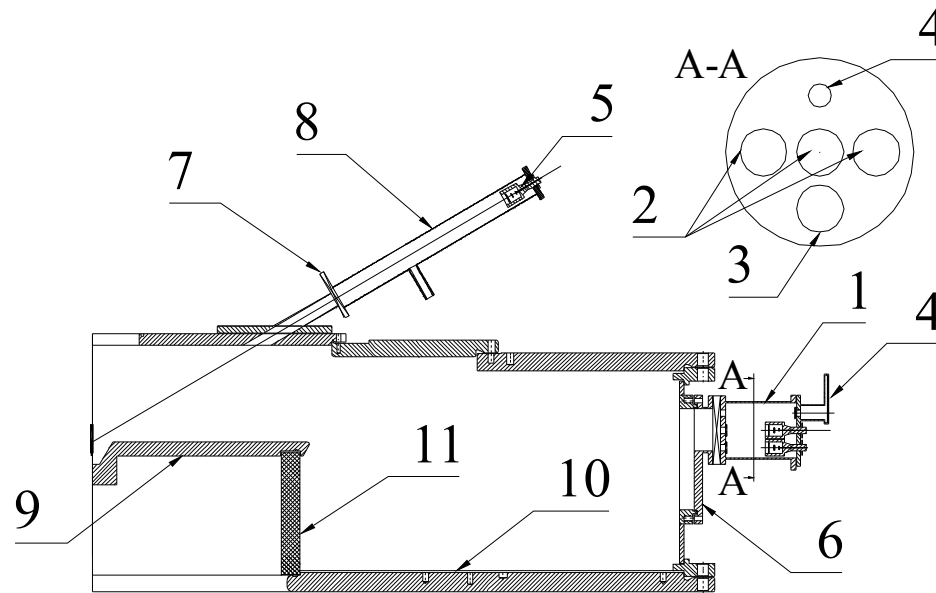
The original design of the central part of the anode has been developed for extracting the radiation from experimental chamber and investigation the interaction of radiation with a substance. Thin ($\sim 1 \mu$) Al and Cu foils evaporation has been achieved.

By calculation of the energy necessary for evaporation of these foils, the estimation of the total SXR yield was done.

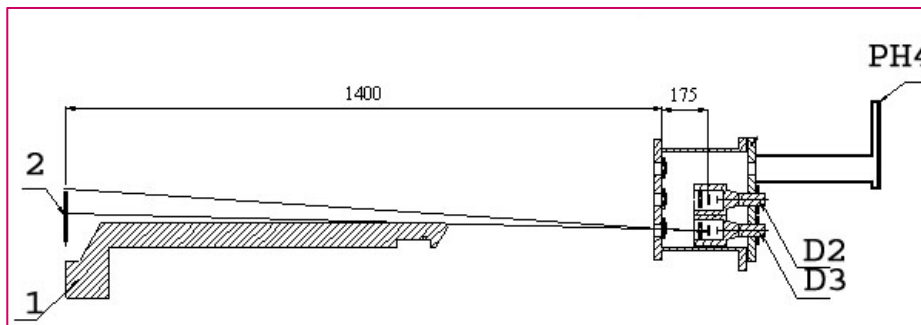
SXR yield up to 100 kJ was obtained at $W=1\text{MJ}$

N.V.Filippov et al., Phys. Lett. A 211 (1996), 168-171

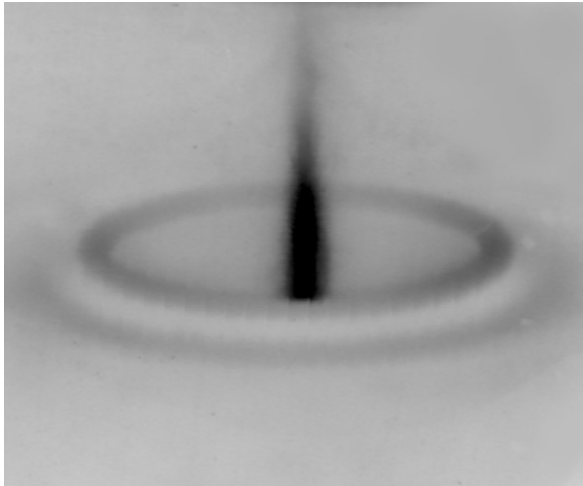
Diagram of X-ray measurements



1 – main detector unit; 2, 3, 5 – pin-diodes, 4 – pin-hole camera; 6, 7 – diagnostic ports, 8 – transitional tube, 9 – anode, 10 – cathode, 11 – insulator.



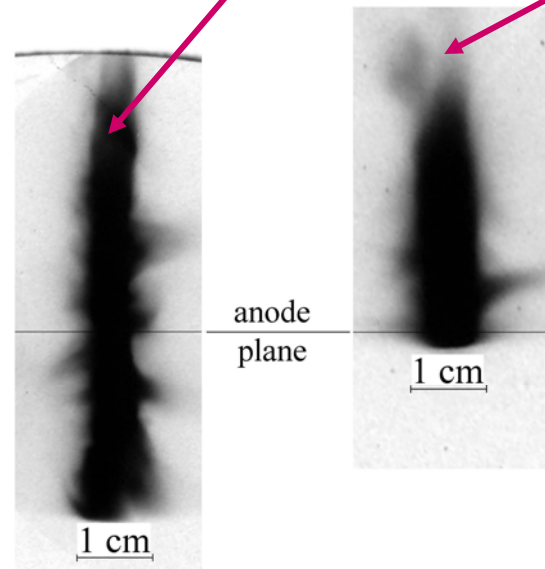
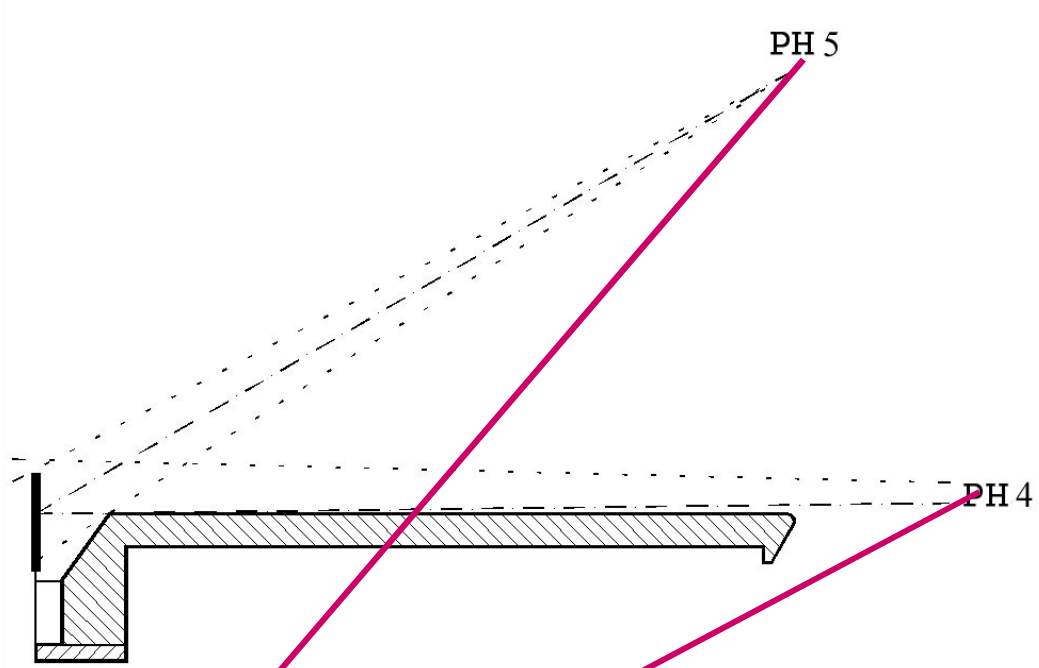
V.I.Krauz et al., 34th EPS Conf. Warsaw, ECA Vol.31F, P-1.021 (2007)



Pinch image produced with the pin-hole camera (PH5) and obtained in 30 sequential shots. One can see very good pinch reproducibility in a space

The considerable part of the pinch is in the conical cavity in the anode below the anode plane →

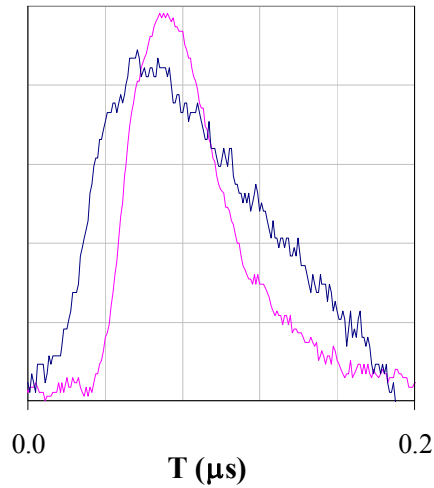
*PH5 (60°)
diaphragm 0.2 mm
filter Be 17 μm;*



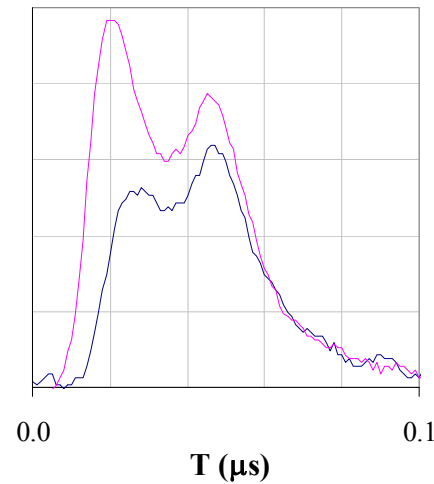
*PH4 (90°)
diaphragm 0.4 mm,
filter Be 10 μm.*

Neon, P = 1 Torr, W=540 kJ

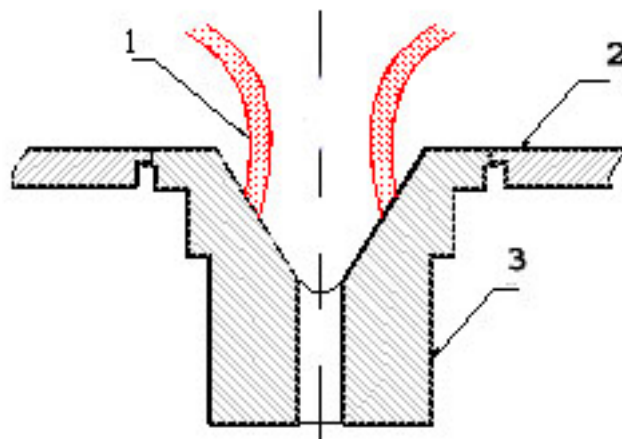
Temporary analysis of signals of pin-diodes D2, D3 and D5 has shown that pinching first takes place in the deepening of the anode and only then, due to zipper-effect, pinch occurs above the anode surface



*Pin-diode signals:
red beam –detector D2 (90°)
blue beam –detector D5 (60°)
Filter Al 8 μm*



*Pin-diode signals:
red beam –detector D2 (90°)
blue beam –detector D3 (90°)
Filter Al 8 μm*

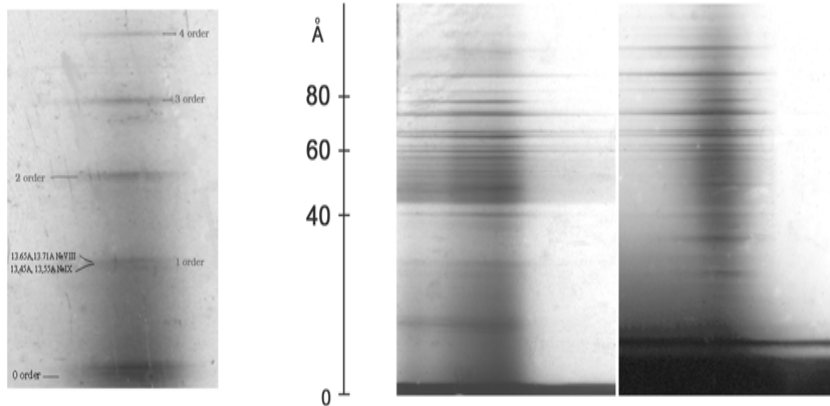


*1 - plasma-current sheath,
2 - anode plane,
3 - conical deepening in the central anode insert*

X-ray spectral measurements

Spectral structure of Ne radiation studies in the range $10 \div 100 \text{ \AA}$ were performed with a grazing-incidence spectrograph, having a concave diffraction – golden covered – lattice replica ($R = 1 \text{ m}$, 1200 lines/mm).

The main problem is low-energy radiation absorption in ambient gas (Ne)

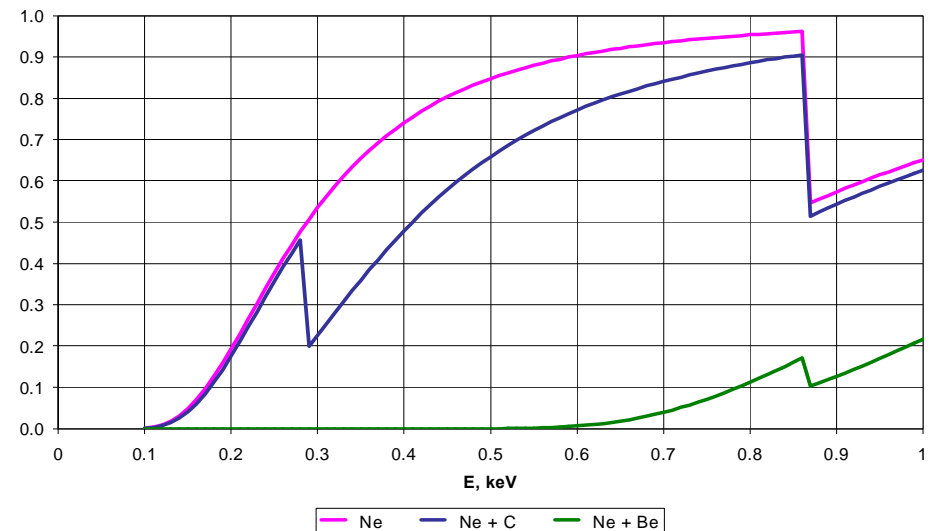


Be, 10 μm ,

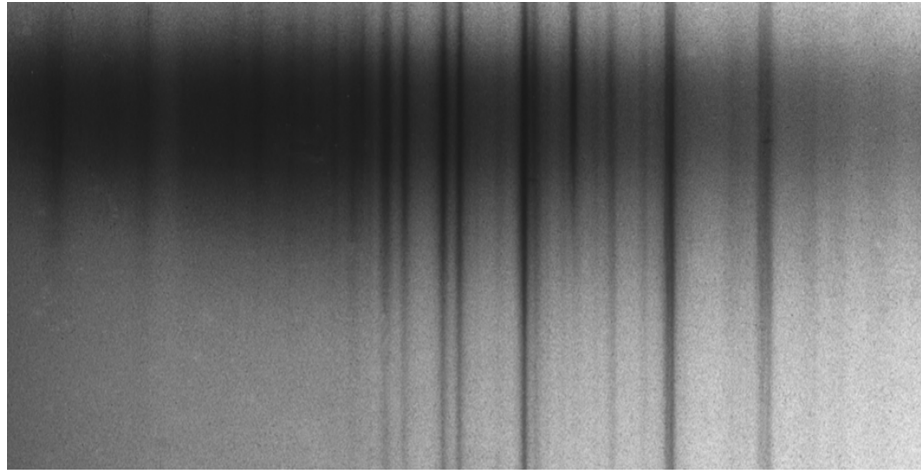
C, 10 μm

*Without
filter*

**W = 450 kJ, P = 1 Torr Ne,
Distance to the pinch – 50 cm, 5 shots**



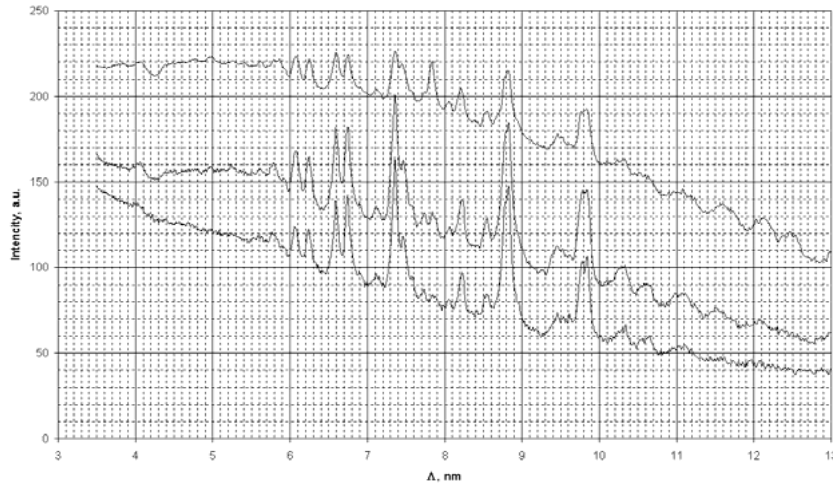
Filters transmission



Spectrogram obtained for 6 shots at P=1 Torr and spectrograph disposition at 60° to the system axis

b)

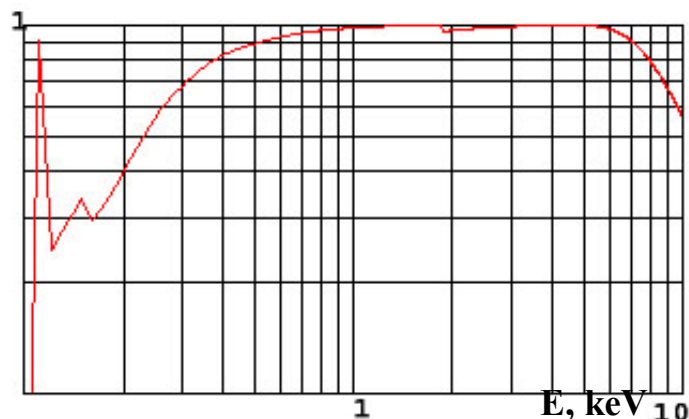
10.3 nm Ne VIII
 9.82 nm Ne VIII
 8.81 nm Ne VIII
 8.5 nm Ne VII
 8.22 nm Ne VII
 7.83 nm Ne IX
 7.46 nm Ne VIII
 7.35 nm Ne VIII
 6.74 nm Ne VIII
 6.59, 6.63 Ne VIII
 6.24 nm Ne VIII
 6.06 nm Ne VIII
 4.37 nm Carbon K-jump



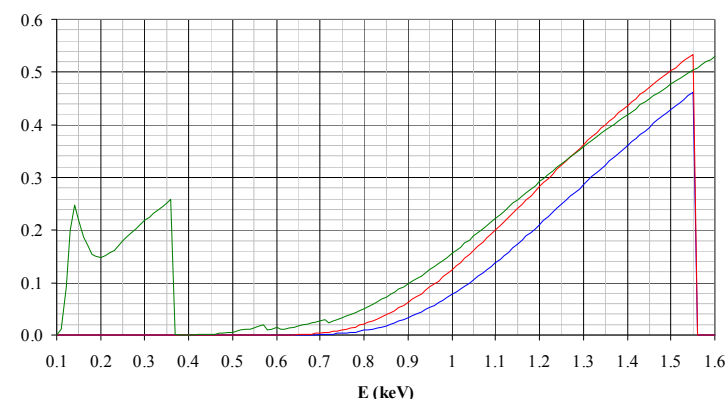
Densitogram of this spectrum: the upper, middle and lower curves show a spectrum on distances 0; 4.5 and 9 mm from the pinch axis, respectively

Pin-diode Spectral Characteristics

For estimation of long-wave radiation contribution to the total SXR yield two open Pin-diodes with Ag and Al filters have been used



Relative spectral sensitivity of open pin-diode, RPPD-11-type

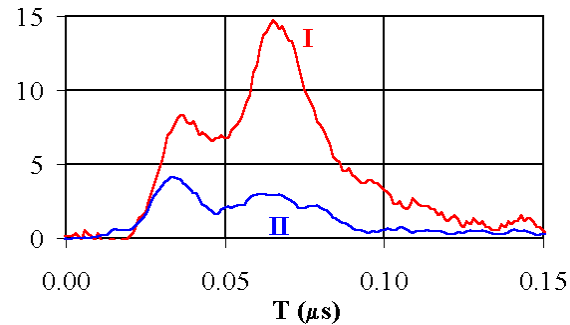


*Pin-diode sensitivities with different filters:
—Al 8 μm , —Al 6.5 μm , —Ag 0.25 μm*

Pin-diode with the filter Ag has high sensitivity in the range of 100 – 350 eV, and the sensitivities of both detectors in the range between 400 eV and 1.5 keV approximately coincide. A difference in the sensitivity at the energy higher than 1.5 keV is not essential, since the absence of noticeable radiation in this spectral range has been shown in our previous experiments. So the energy range of interest (100 – 350 eV) can be estimated as a difference in the detector signals.

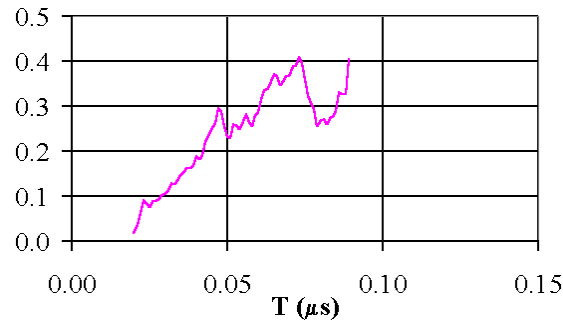
SXR Studies in Time

*P=1 Torr, neon,
W=160 kJ
I – filter 8 μm Al
II – 0.25 μm Ag*



Two well-pronounced peaks in X-ray pulses are characteristic for operation at 1 Torr and at not very high bank energy

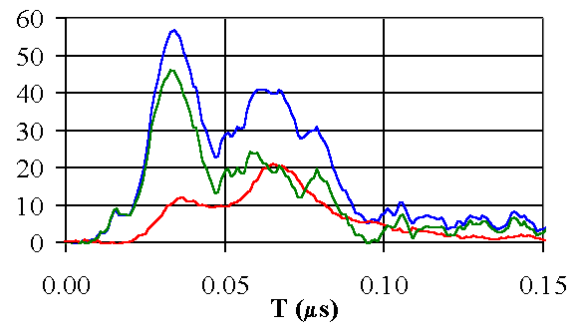
Signals ratio at taking into account the condition of registration



Radiation hardness increases during the pulse. But “effective” energy of radiation at each instant is lower than 1 keV. This effect can be caused by presence of the long-wave radiation.

“Recalculated” signals:

*— Al 8 μm ;
— Ag 0.25 μm ;
— signals difference*



The radiation in the range of 100-360 eV makes up to 70 % of the total yield.

Precise calculation of energy radiated by the pinch is difficult because of unknown working gas distribution in the vacuum chamber.

Current distribution and current-carrying plasma sheath dynamics

Dependence of the pinch plasma and radiation parameters on the discharge current is one of the key problems in the pinch systems studies.

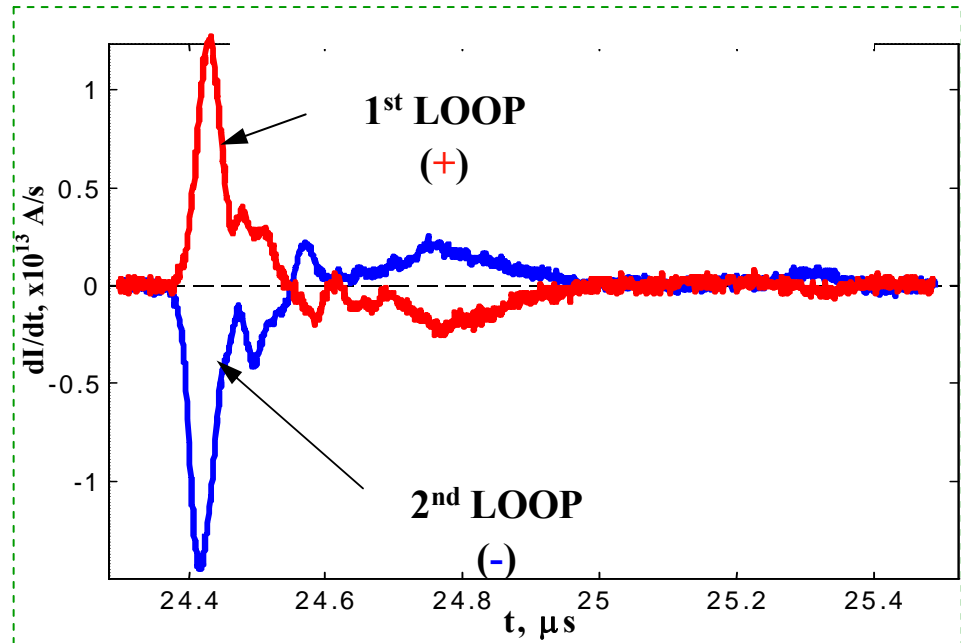
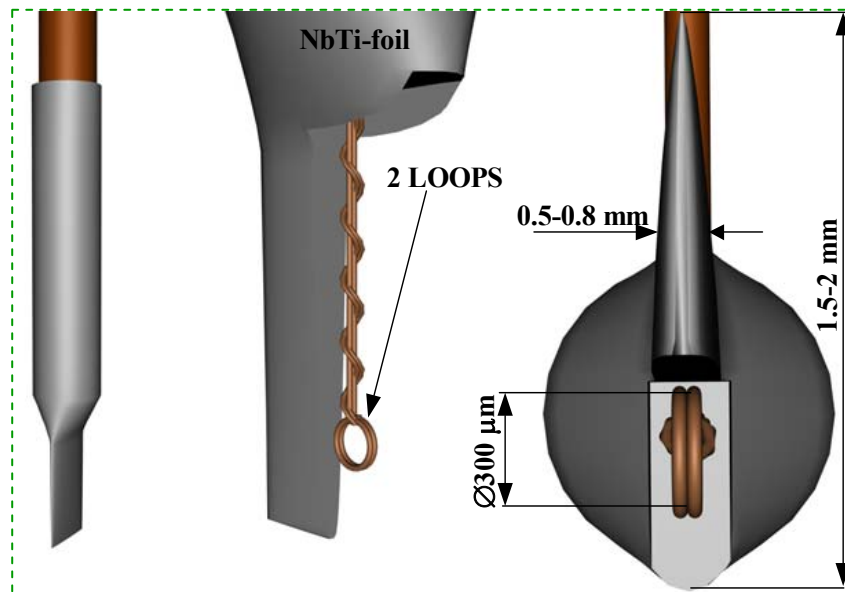
Current spatial distribution influences essentially on the processes of the magnetic energy dissipation and on the mechanisms of the radiation generation.

This problem takes on a special significance in the studies of the plasma focus-type facilities because of the important role in the discharge dynamics the so-called “preparatory stages”, which are responsible for efficiency of transferring the current to the pinch area.

Importance of this problem grows sharply at increasing the discharge energy.

In particular, one of the possible reasons of the observed violation of the neutron scaling on the Mega-Joule-range facilities may be a shunting of the pinch current by the residual plasma on the discharge periphery.

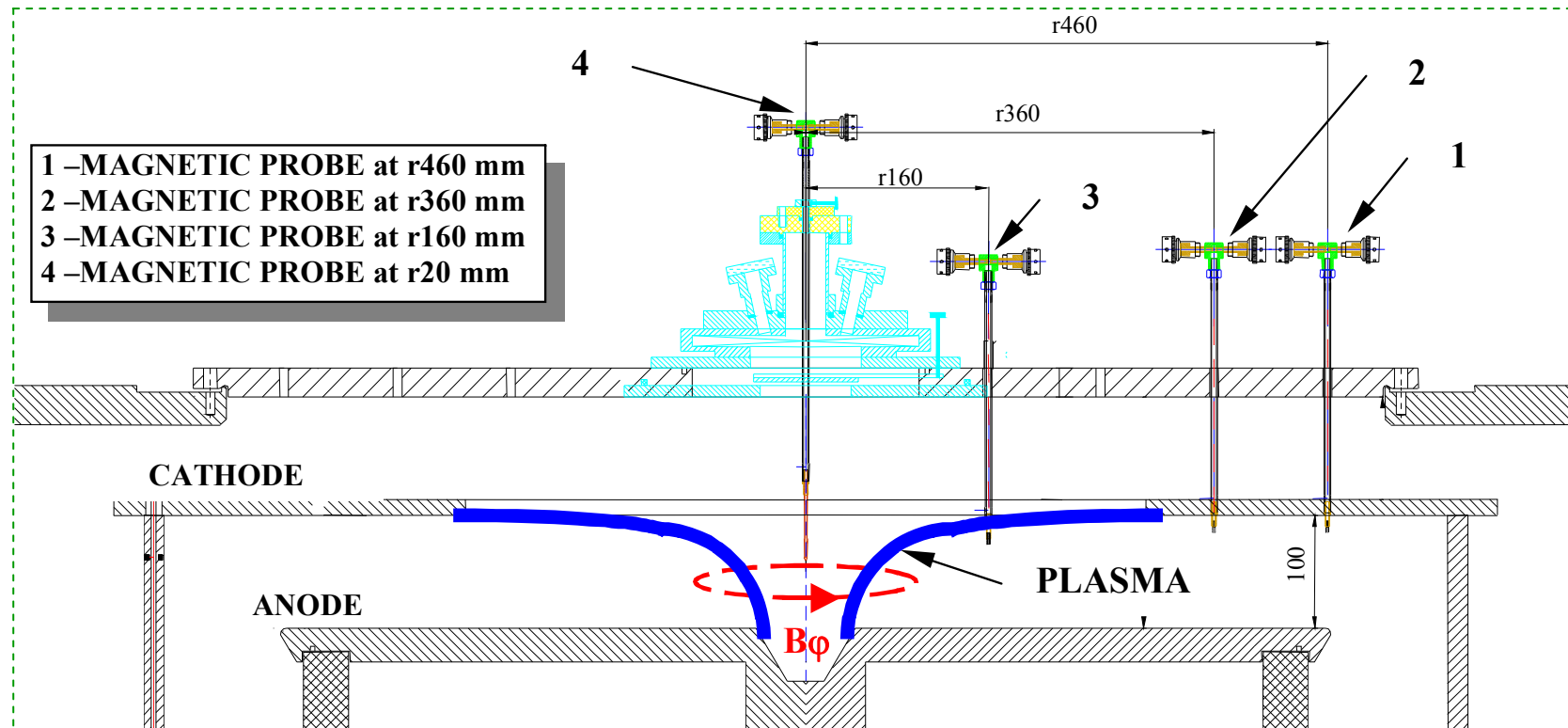
TECHNIQUE OF MAGNETIC FIELDS MEASUREMENTS



E. Grabovsky, G. Zukakishvili, K. Mitrofanov, et al. In Advanced Diagnostics for Magnetic and Inertial Fusion. Edited by P.E. Stott et al., Academic/Plenum Publishers. 2001, p. 257

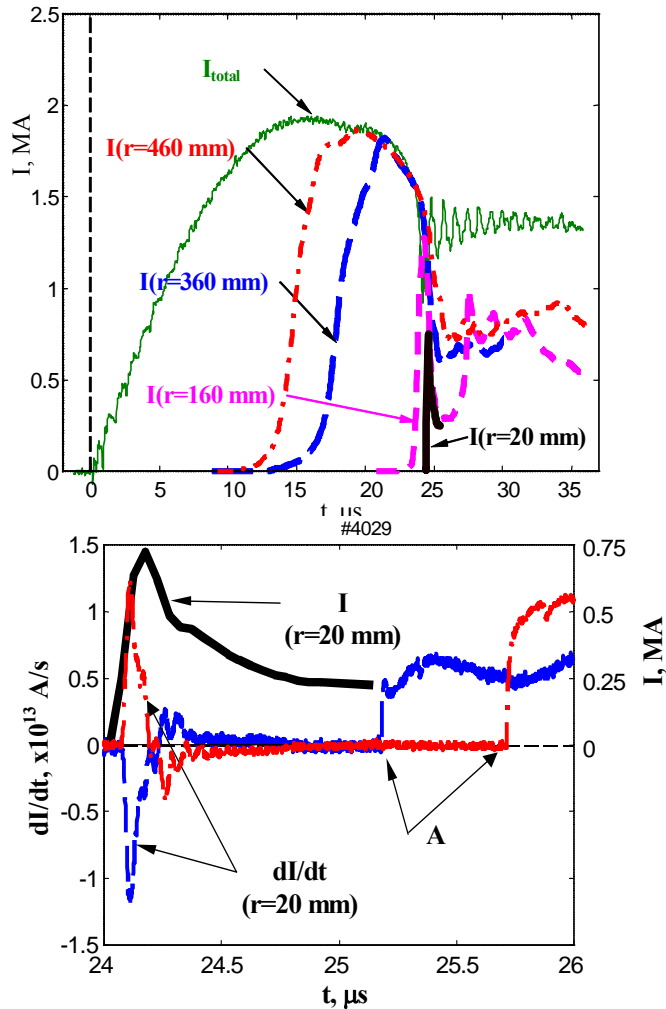
- The absolutely calibrated magnetic probes have been designed for the measurements of the plasma current sheath parameters.
- The probes consist of two loops, 300 μm in diameter, in a common screen of NbTi-foil 10-15 μm thickness.
- It provides two signals with different polarity from each probe. It allows to pick out the pulses having magnetic nature. \Rightarrow Probe signal $U_p \sim dB/dt \Rightarrow B \sim \int U_p(t) dt \Rightarrow I \sim B \cdot r$

EXPERIMENTAL SETUP:



- Special units with vacuum lock has been developed for installing the probes on various distances along the radius and on different height above the anode without vacuum violation in the chamber.
- The measurements with simultaneous use of several probes located at radii $r=460$ mm, 360 mm, 160 mm and 20 mm were carried out.
- Experiments were performed at the power supply energy $W = 290$ kJ with argon and neon as working gases at the pressure of 1.5 Torr.

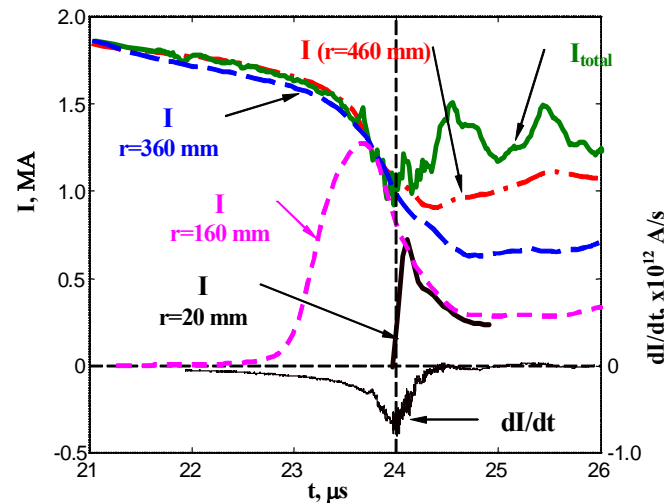
STUDIES OF THE AZIMUTHAL MAGNETIC FIELDS



Signals from probes coincide with the total current after the PCS passes the probe.

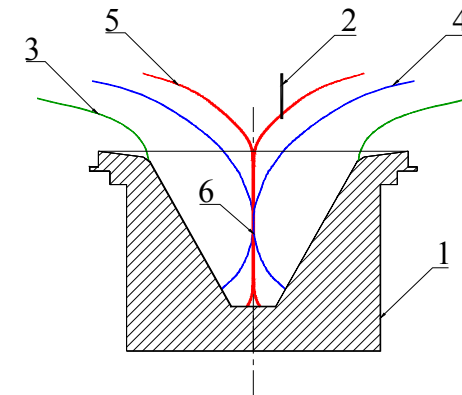
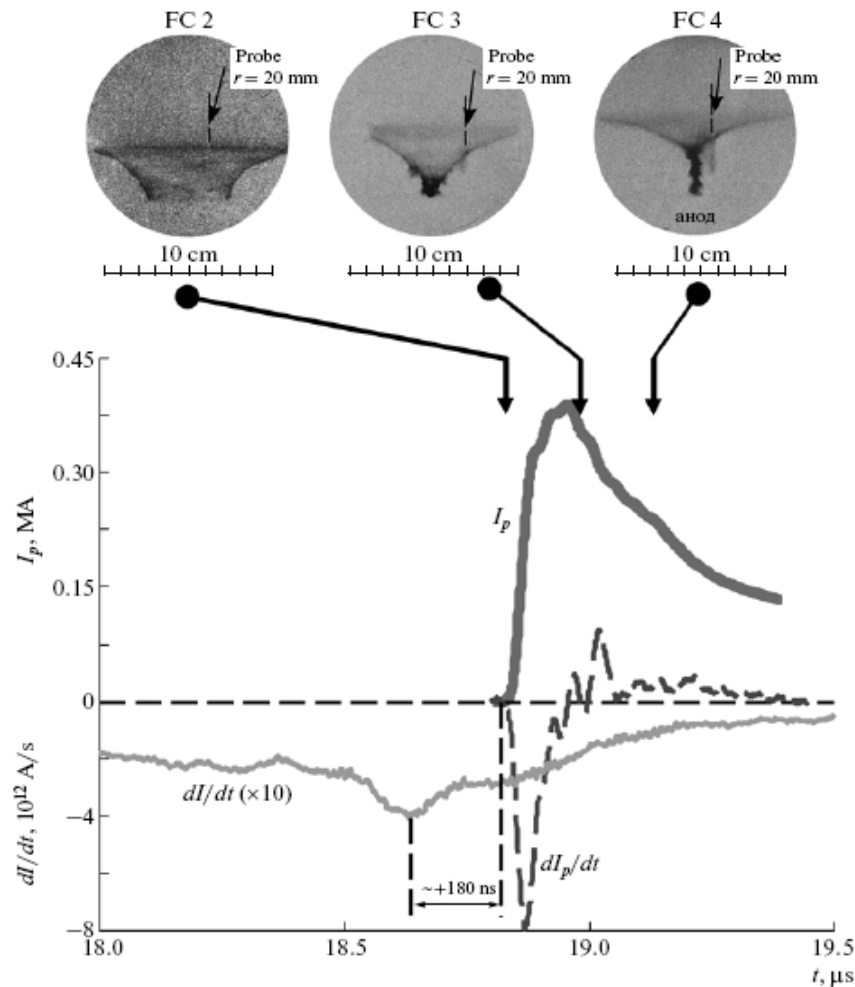
The current efficiently transfers toward the axis!

After the "peculiarity" $\approx 40\%$ of the current flows outside of the zone with $r=460$ mm (nearby insulator).



Current measured by probe at $r = 2$ cm is as low as 0.8 MA. However, its amplitude coincides with the current value measured by probe at 16 cm at the same instant and the subsequent behavior of these currents being identical. Due to its noncylindrical shape, the CS reaches probe, located at a height of 1 cm over the anode plane, after the beginning of pinch formation inside the conical cavity

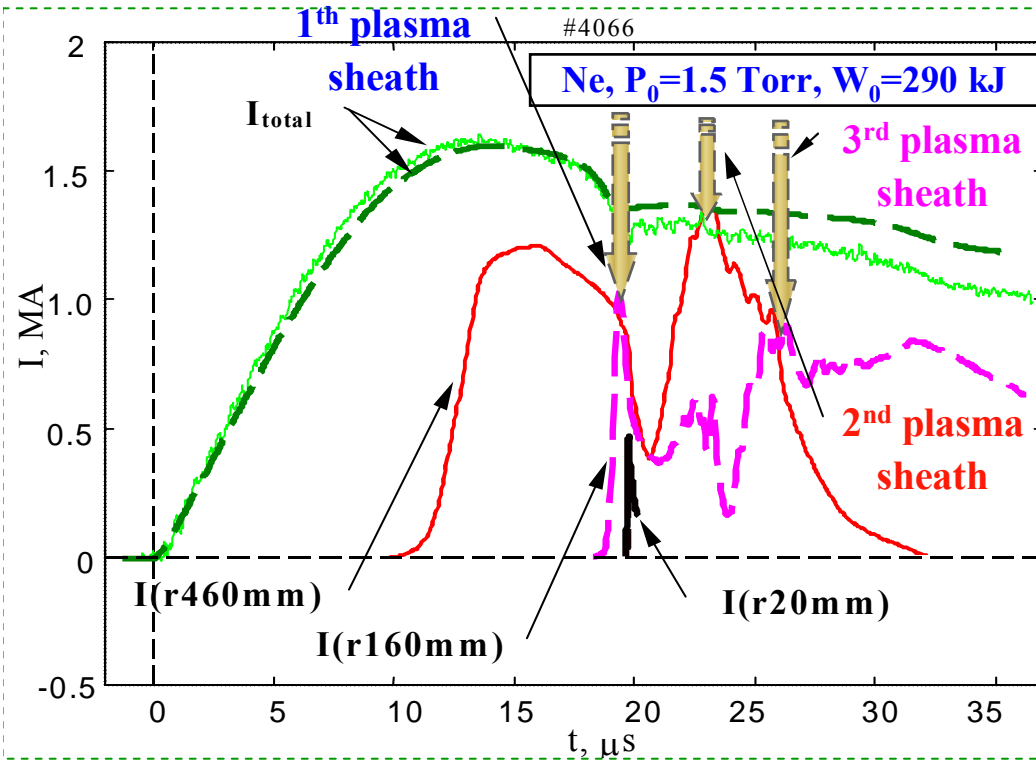
Scenario of pinch formation inside the conical cavity of the anode



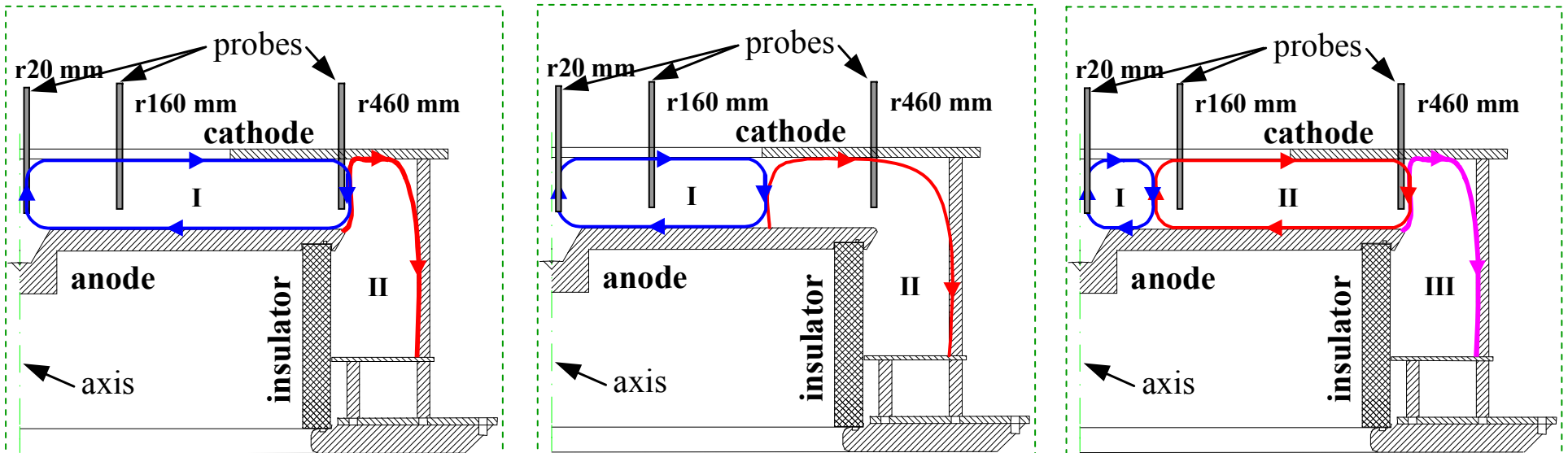
(1) conical cavity, (2) magnetic probe, (3) shape of the CS at the instant at which it arrives at the edge of the conical cavity, (4) shape of the CS at the beginning of its collapse onto the axis, (5) shape of the CS at the instant at which it passes probe, and (6) origin of pinch formation.

Small value of the current measured by a probe can be caused both by the current dissipation in the pinch phase and switching the current to the peripheral areas of the discharge

CURRENT LOOPS FORMATION



- In this case not all current leaves the insulator area from the very beginning of the discharge.
- Magnetic probes at r460 mm and at r160 mm register the currents in different current circuits.



These results allow us to formulate two important conclusions:

➤ *At currents of up to ~2 MA, almost the entire discharge current can be transferred to the axial region. This conclusion is very important for estimating the prospects and capabilities of future high-current PF facilities.*

➤ *However this result is not trivial, because the efficiency of current transfer depends strongly on the operating mode of the discharge. Taking into account that the PF emission parameters depend strongly on the pinch current, the problem of measuring this current is very challenging.*

*New approaches
in PF studies*

Laboratory simulations of super-Alfvenic shocks in a weakly ionized medium

The main goal of these especially designed experiments was to provide data for testing numerical models, in order to better understand the interaction of a high-velocity plasma jet with a partially ionized gas in a strong transversal magnetic field.

✓ At PCS compression to the axis the generation of cumulative plasma jets driven along the axis with a velocity $\sim 10^7$ cm/s takes place.

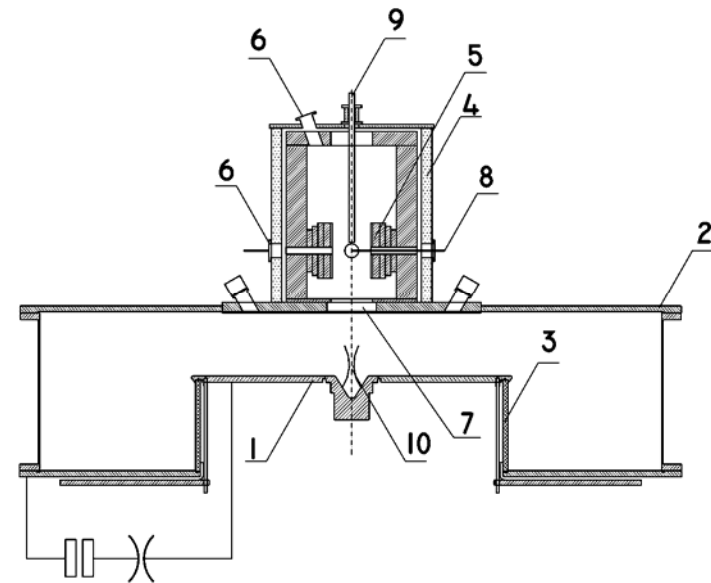
✓ This directed driving is realized in the ambient plasma arisen as a result of the working gas ionization by the X-ray radiation of the plasma focus.

✓ The transversal magnetic field up to 2500 G was created in the chamber of interaction by the magnetic system based on rare-earth magnets.

✓ The experimental conditions allowed us to perform experiments with Alfven Mach number $MA \geq 3$.

N.V.Filippov et al., Nucleonika 2001; 46 (1)

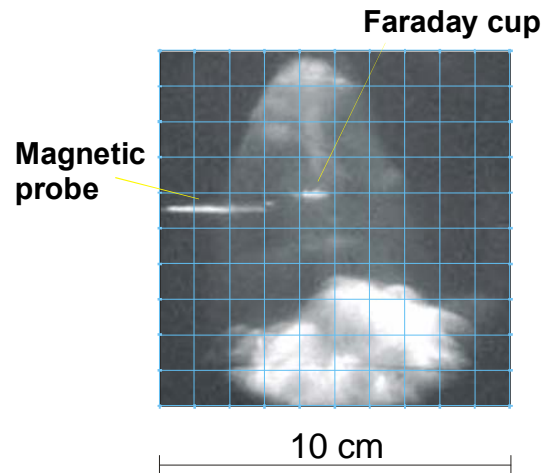
N.V.Filippov et al., Czech. J. Phys. 50/S3, 2000



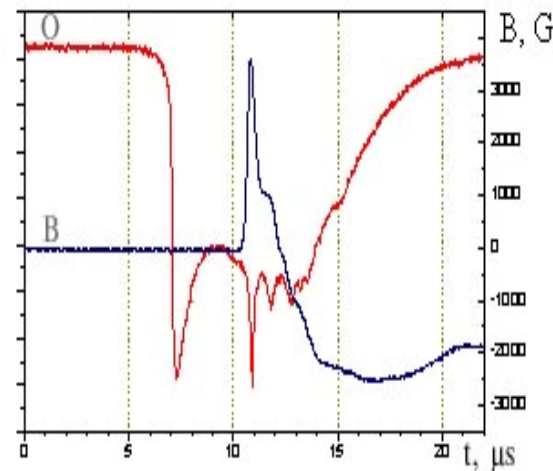
1 – anode; 2 – cathode; 3 – insulator; 4 – chamber of interaction; 5 – magnetic poles; 6 – diagnostic ports; 7 – mesh; 8 – magnetic-optical probe; 9 – Faraday cup; 10 – pinch.

Kurchatov Institute, CEA (France)

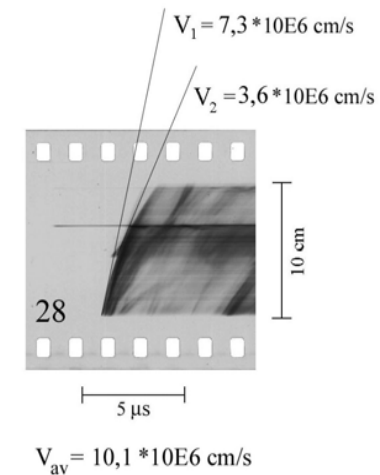
$W \sim 1 \text{ MJ}$, $I \sim 3 \text{ MA}$, $P_{\text{Ne}} = 0.5 \div 1 \text{ Torr}$, $B_0 = 2500 \text{ G}$, $M_A = 3 \div 10$



Plasma jet image
 $\tau_{\text{exp}} = 10 \text{ ns}$



Traces of the magnetic (B) and optic (O) probes



Plasma jet deceleration
 $M_A = 4.5$

Observed magnetic field compression, plasma density profile evolution, and shock slowing down, are well reproduced by a two-dimensional hybrid code HAWAI2D

D.Mourenas et al., Physics of Plasmas; Vol.10, No 3, 2003

PLASMA FOCUS AS A DRIVER FOR THE MAGNETIC COMPRESSION OF LINERS

The usage of the PF-type facilities as current generators can be a rather promising direction that is related with an opportunity to produce an comparatively simple and cheap engineering laboratory devices for studies in the physics of high energy densities.

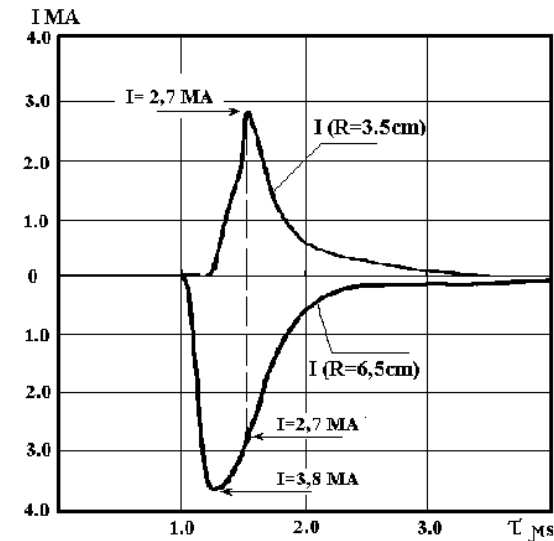
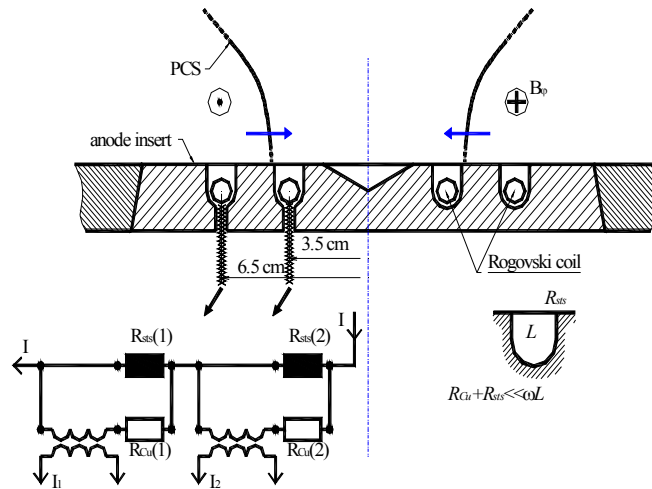
The combined circuit-diagrams are discussed for creating laboratory soft X-ray radiation sources, where PF are used as inductive storage and the current sheath realizes the transport of its energy to the load placed at the system axis.

M.Scholz et al., Phys.Lett., A 262 (1999), 453-456
V.I.Krauz, et al. Int. Symp. PLASMA-2001, 2001, I3-1

This scheme allows one to perform modeling studies of the compression of different liner loads using in the fast Z-pinch experiments.

Spatial Current Peaking

N.V. Filippov et al, Current Trends in International Fusion Research, 2nd Symposium, Washington, 1997



At the real accessible parameters $I \sim 3 \text{ MA}$, $\delta \sim 1 \text{ cm}$ и $V_r \sim 3 \cdot 10^7 \text{ cm/s}$, it is possible to achieve current increasing rate on the load

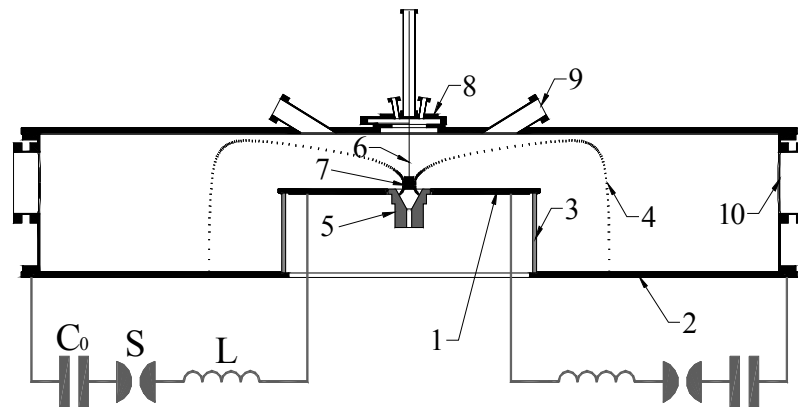
$$\dot{I} \sim I (V_r / \delta) \sim 10^{14} \text{ A/c}$$

The main problem: the efficiency of the energy transfer to the load

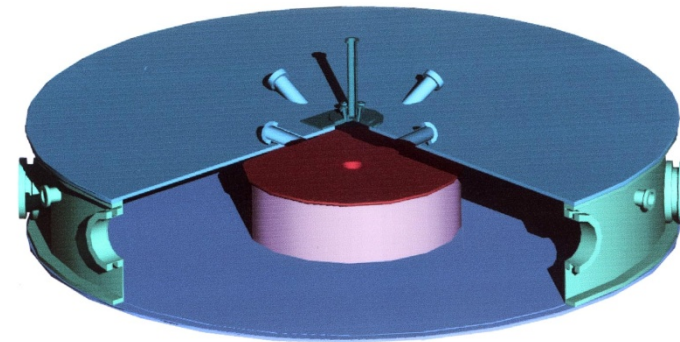


Experimental Setup for Experiments with Liners

Special unit with a vacuum lock has been developed for the delivery of liners to the compression zone. Depending on the type of the used load (liners, fibers, dust) various modifications of the loading unit were applied.



1 – anode; 2 – cathode; 3 – insulator; 4 – plasma current sheath; 5 – anode insertion; 6 – suspension ware; 7 – liner; 8 – loading unit with a vacuum lock; 9, 10 – diagnostics ports;



PF discharge chamber

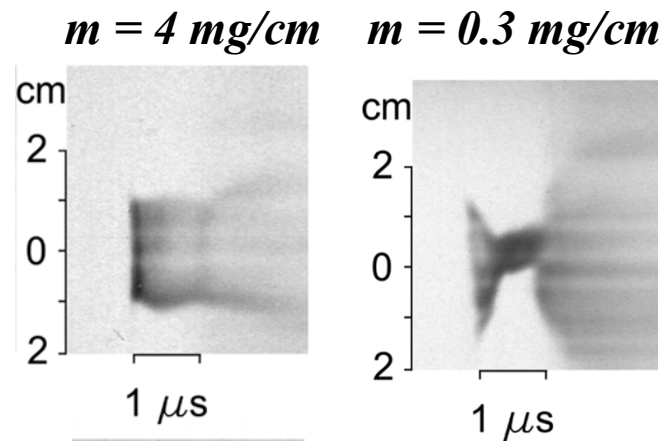
Foam Liner Compression

Thin-walled agar foam liners, 20 mm in diameter, linear mass 0.3 - 4.0 mg/cm

$$I_{\text{pinch}} = 1.2 \text{ MA}, P_0 = 1 \text{ Torr Ne}$$

(*M.A.Karakin et al., Czech. J. of Phys., Vol.52, Suppl.D (2002), 255-263*)

Streak-camera

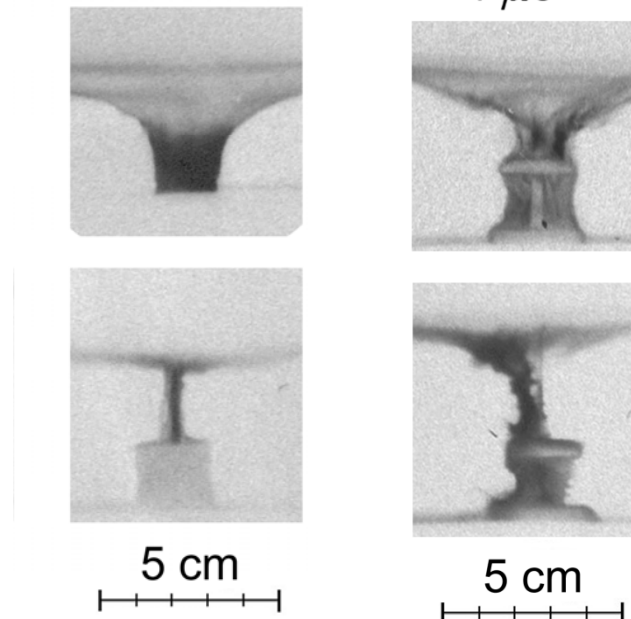


Main result:

Easy (0.3 - 0.6 mg/cm)
liners compression with
velocity $\sim 3 \cdot 10^6$ cm/s

frame camera

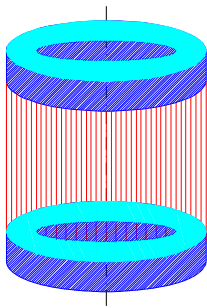
$\Delta\tau=150 \text{ ns}$



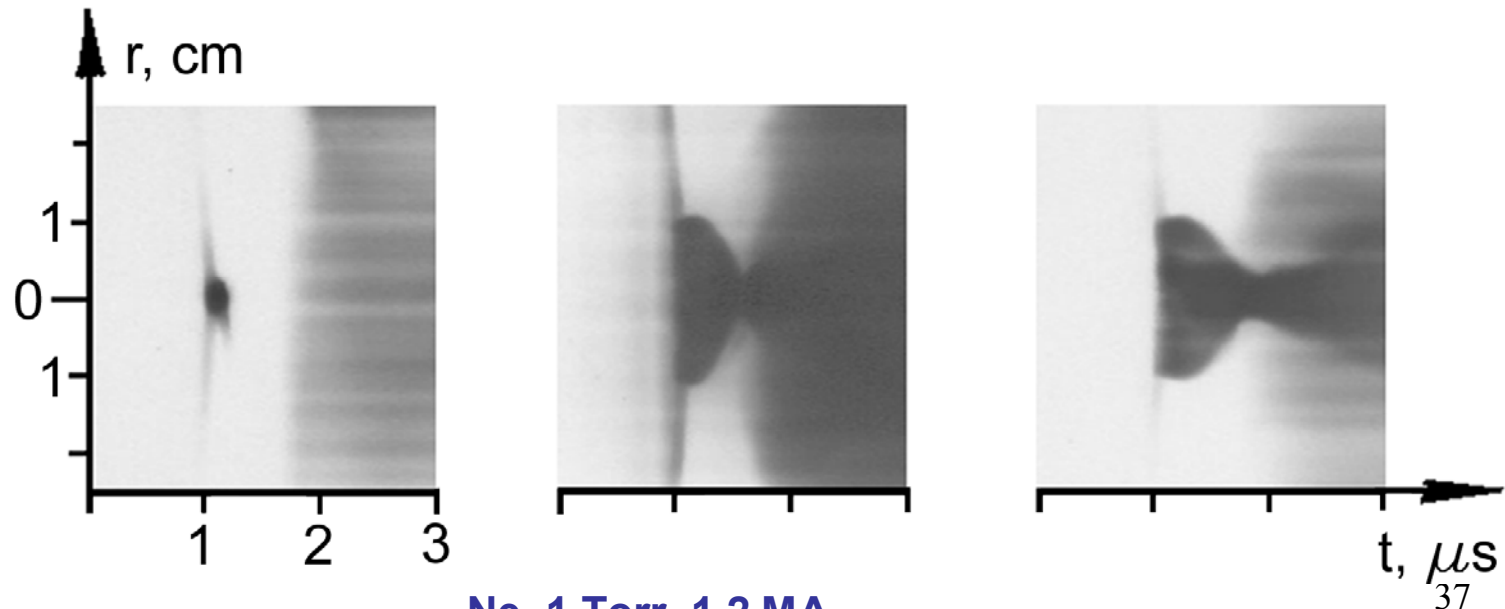
Wire Array Compression

Streak camera

Dense Z-pinches, 5th Int. Conf. on Z-pinches, Albuquerque, New Mexico, 23-28 June 2002, Melville, New York, 2002, ACP, V.651, p. 37-42

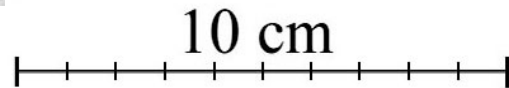
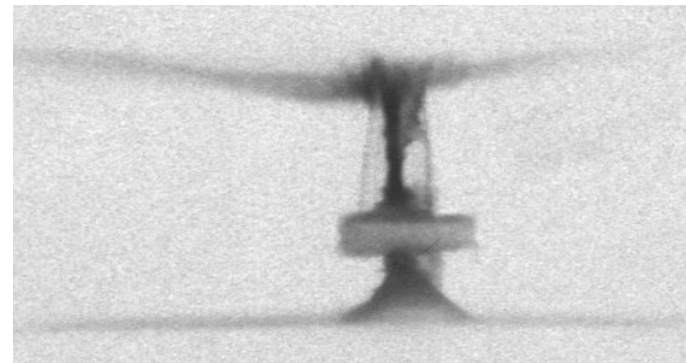
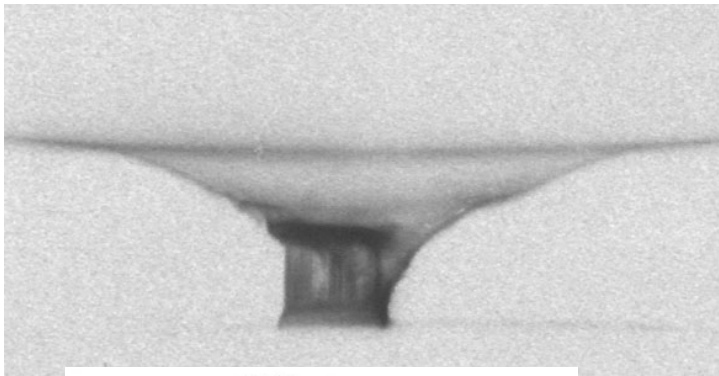
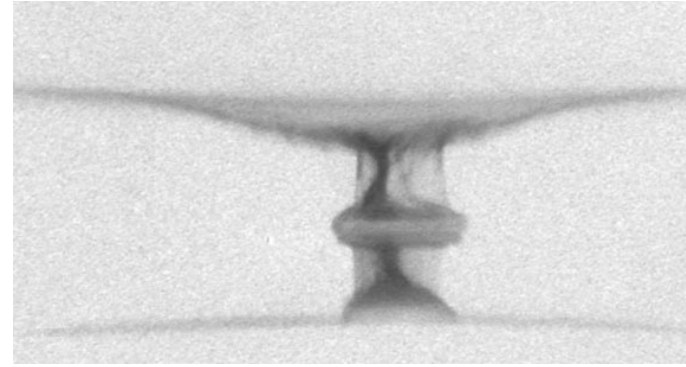
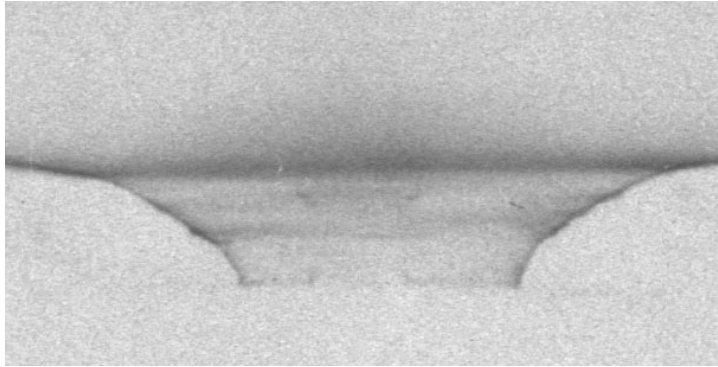


Technology of wire array production has developed at TRINITY: 60 tungsten wires, $6 \div 8 \mu\text{m}$ in diameter, 15 mm long are pulled between two metallic discs along the diameter of 20 mm with a step of $\sim 1 \text{ mm}$



Wire Array Compression

Frame camera

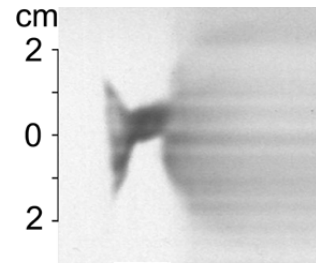


**Ne, 1 Torr, 1.2 MA, Wire array - W, 6 μm , $\text{\O}20$ mm, 330 $\mu\text{g}/\text{cm}$.
Frame exposure - 10 ns, time delay - 150 ns**

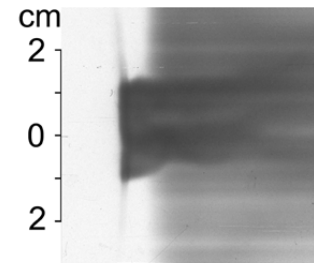
Dependence on Pinch Current

Foam liner

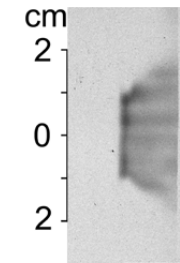
$I_{\text{PINCH}} \approx 1.2 \text{ MA}$



060901_21

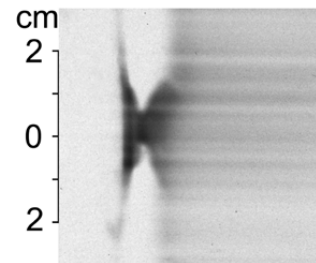


121101_32

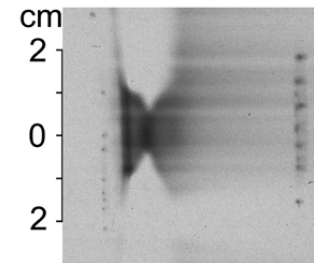


181001_35

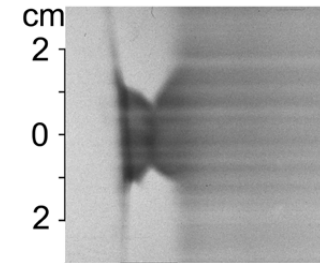
$I_{\text{PINCH}} \approx 2.5 \text{ MA}$



261202_26



201202_13



191202_04

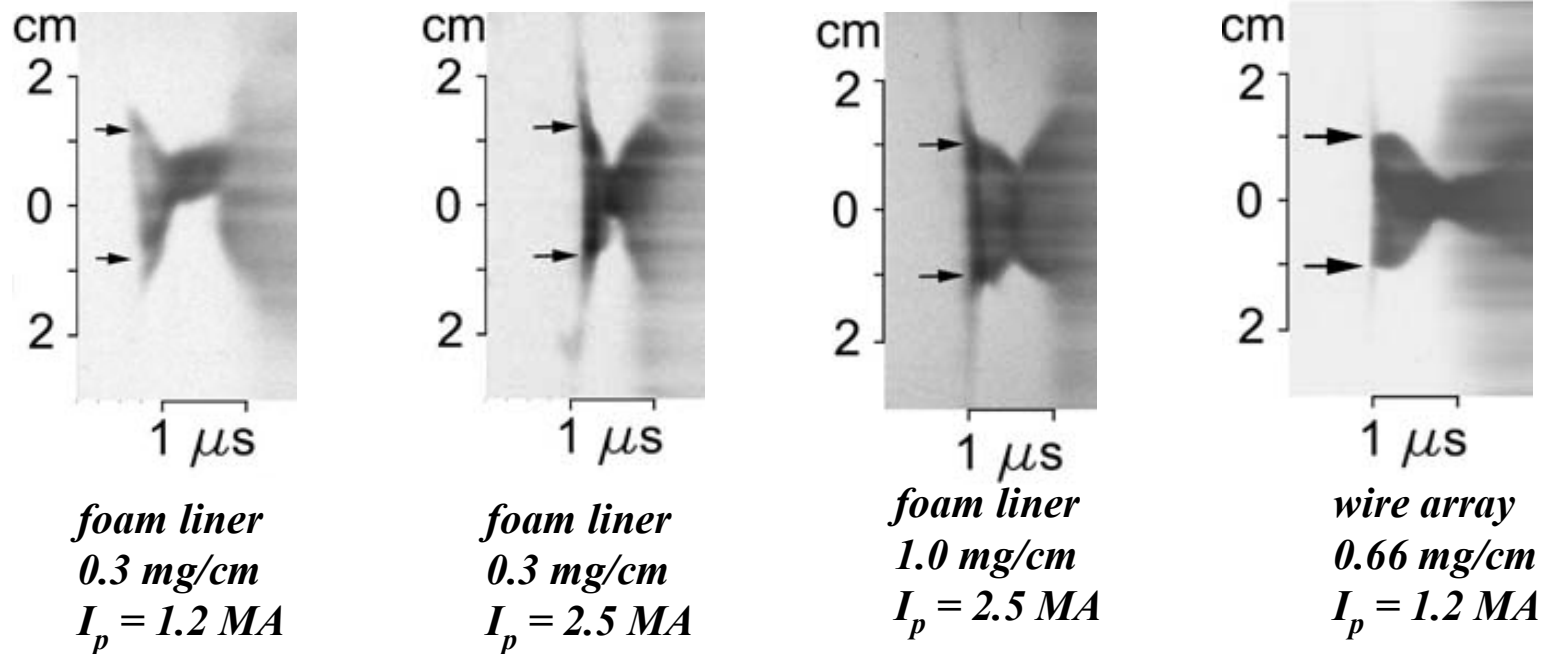
0.33 mg/cm

0.6 mg/cm

1.0 mg/cm

Influence of the PCS Radiation

Distinctive feature of experiments on PF-3 is use of strongly-radiating gases. Under conditions of a long radial compression stage duration ($\sim 10\mu\text{s}$) a preliminary heating of the target located at the axis and acceleration of the initially – condensed material transition into plasma state can be attained (*Plasma Phys. Rep.*, 2008, V. 34, № 1, p. 43)

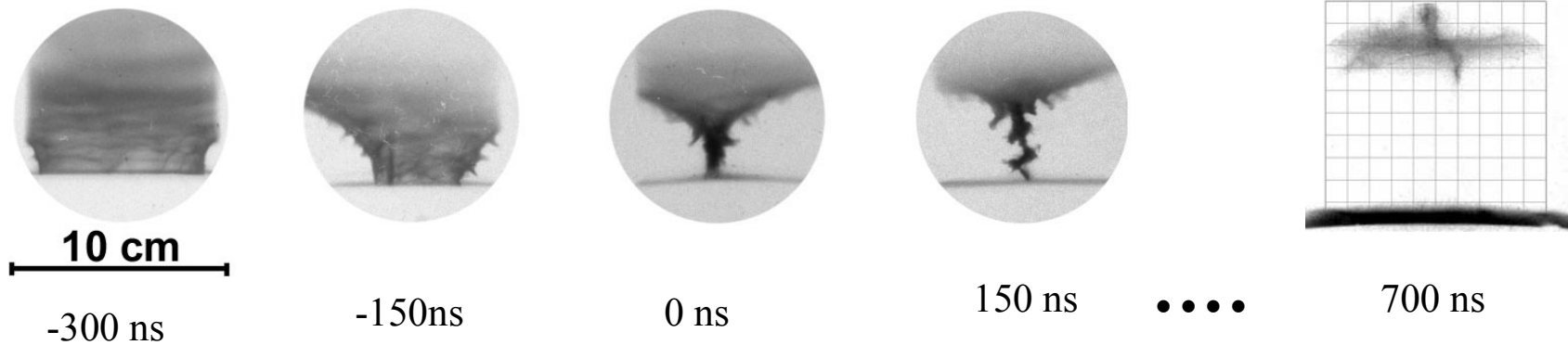


Diameter of the foam liner at the instant of the contact with the sheath exceeds the initial diameter – pre-heating by the sheath radiation. Therefore, one can effectively control over the process of the liner evaporation and ionisation by changing the gas and the liner parameters that assists in **overcoming “cold start” problem.**

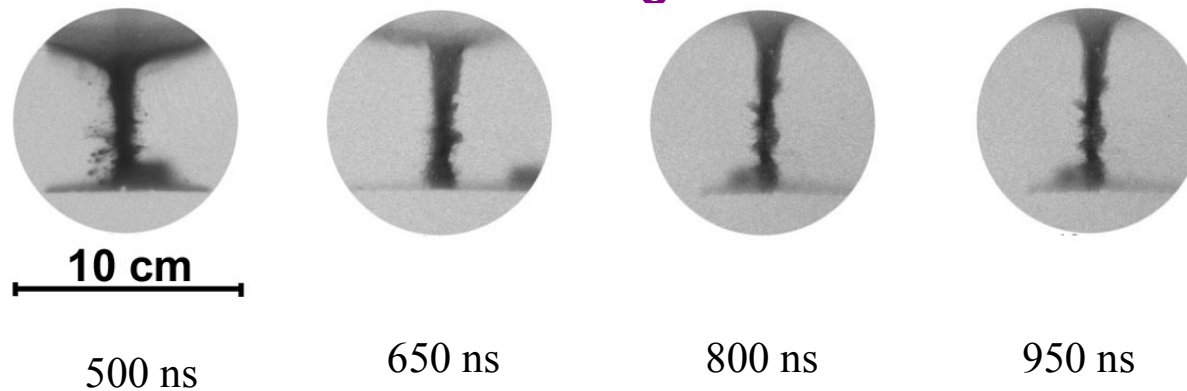
Frame Camera Pictures of Pinch Formation

Frame exposure – 12 ns, time delay between frames – 150 ns

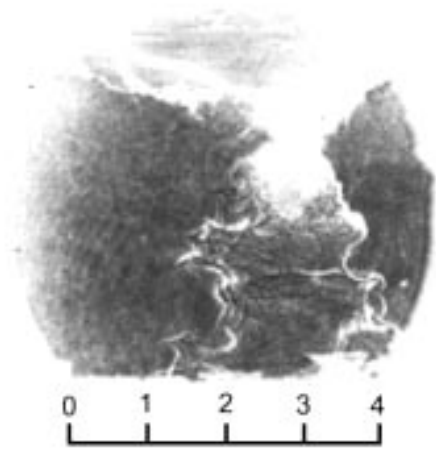
Discharge in neon **without dust**



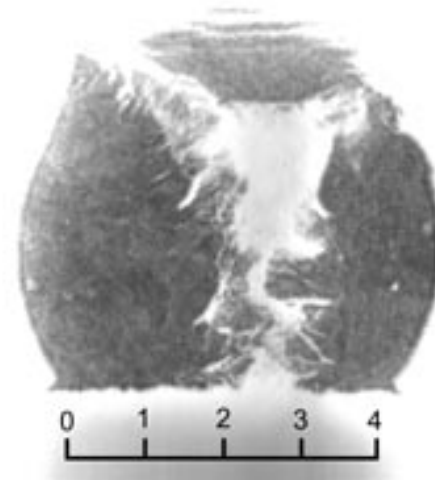
Discharge in neon **with dust**



Shadow pictures



+180 ns, without dust



+ 160 ns, with dust

If in the shot without the dust the sheath scattering is observed without appreciable density in the centre, in “dusty” shot one can clearly see the dense plasma core.

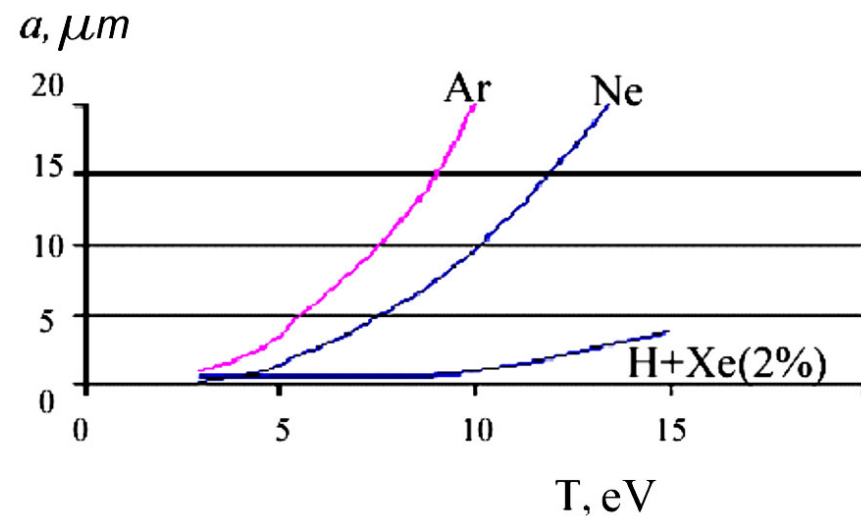
Experiments with dust: *main results*

Due to the volumetric character of grains interaction with plasma and radiation, an effective evaporation and the ionization of grains takes place, providing the presence of the additional plasma sources in the pinch area and “smoothing” the development of MHD-instabilities.

V.I.Krauz et al., Plasma Phys. Rep., 2008, V. 34, № 1, p. 43

It is shown that in the shots with the dust the more stable pinches - relative to the MHD-instabilities - are formed.

Such approach can be promising in respect of production of nanopowders and nanocoatings at microparticles transformation in nanoparticles in a plasma column with the subsequent deposition on substrates



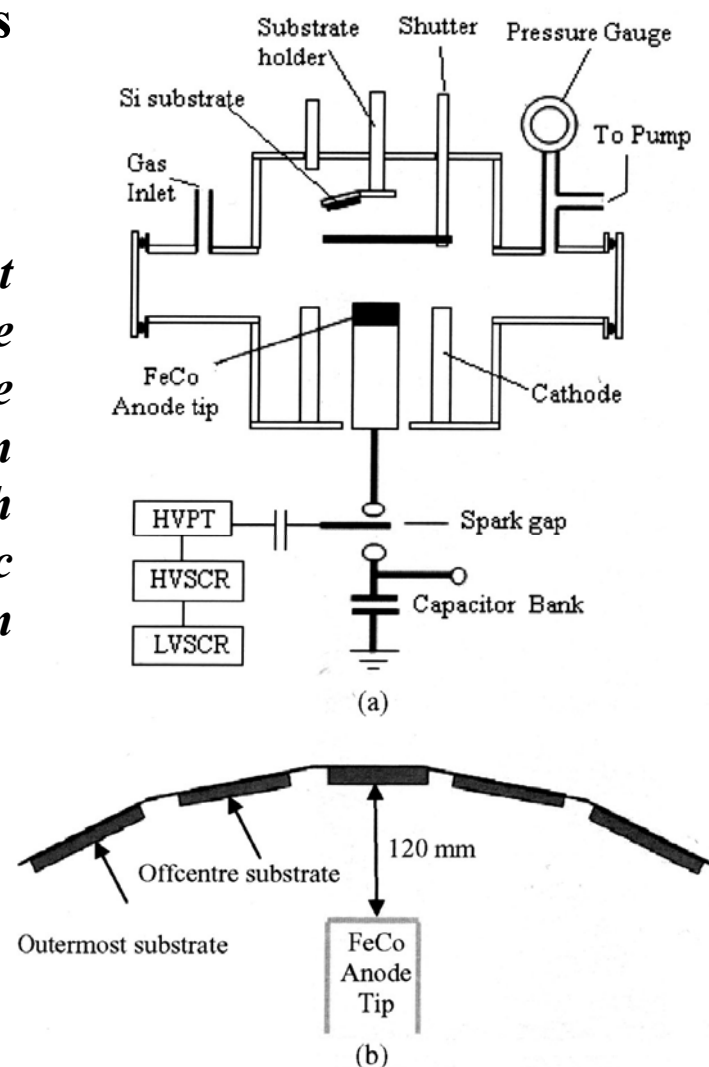
Grains evaporation
depending on sheet temperature

Nano-particles and nano-films in PF

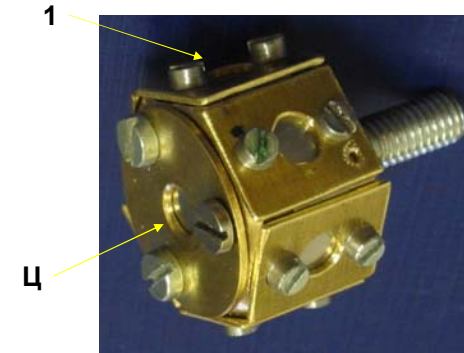
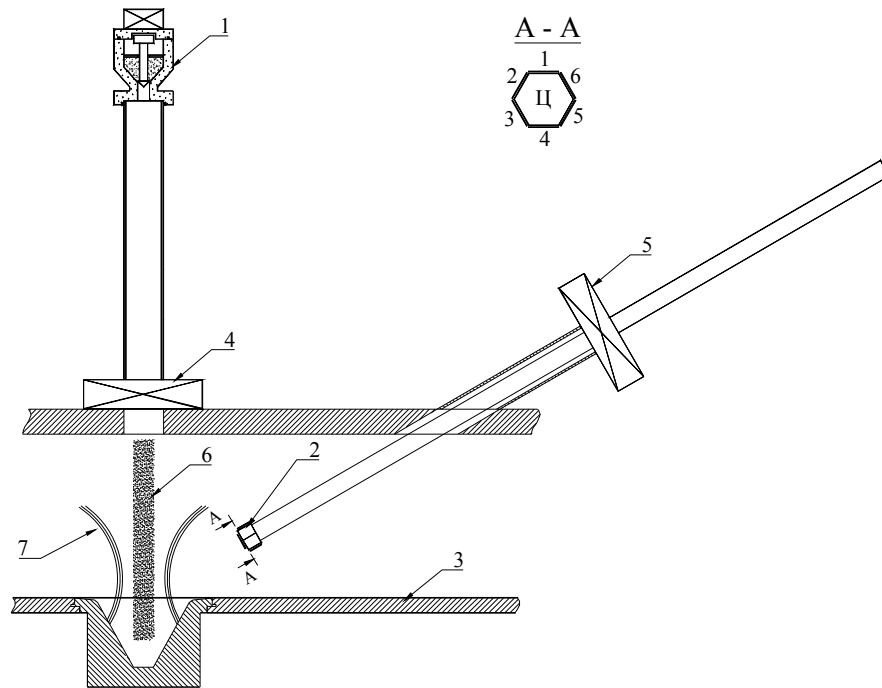
Production of various nano-structures is one of the most intensive directions in PF studies now.

In conventional way such structures arise at ablation of substance, inserted in the anode tip, under the impact of hot plasma and the electron beam with the subsequent deposition on the substrate. This technique has such advantages as high deposition rate, energetic deposition process and possible deposition under a reactive background gas pressures.

*T.Zhang, S.Mahmmod, J.Lin, S.M.Hassan,
T.L.Tan, S.V. Springham, P.Lee, R.S.Rawat
National Institute of Education, NTU, Singapore
33rd EPS, Rome, Vol.30I, P-2.065 (2006)*



Experimental Setup

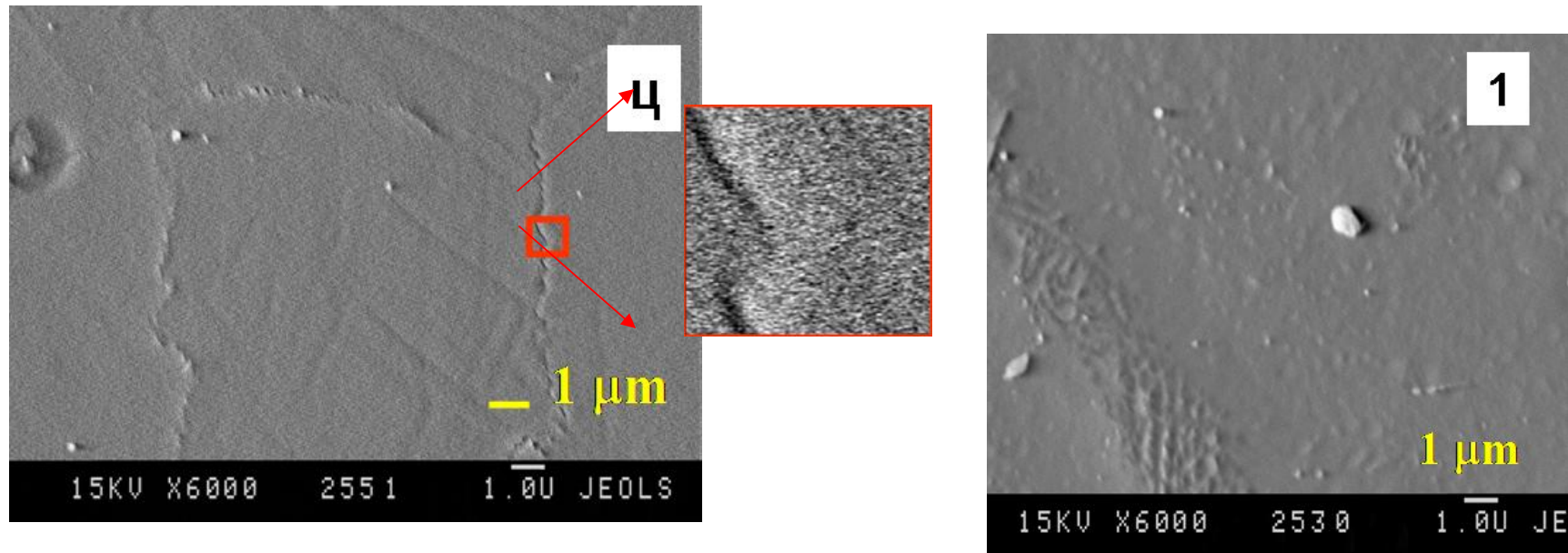


Substrate holder

1 – tank with micro-particles; 2 – substrate holder ; 3 – anode; 4, 5 – vacuum locks; 6 – dust target; 7 – PCS.

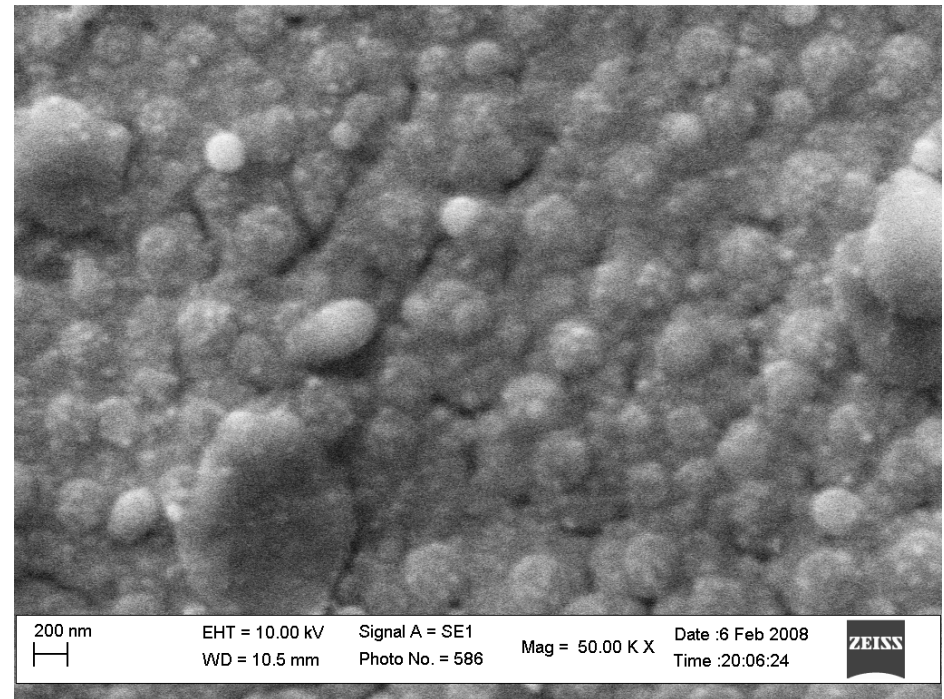
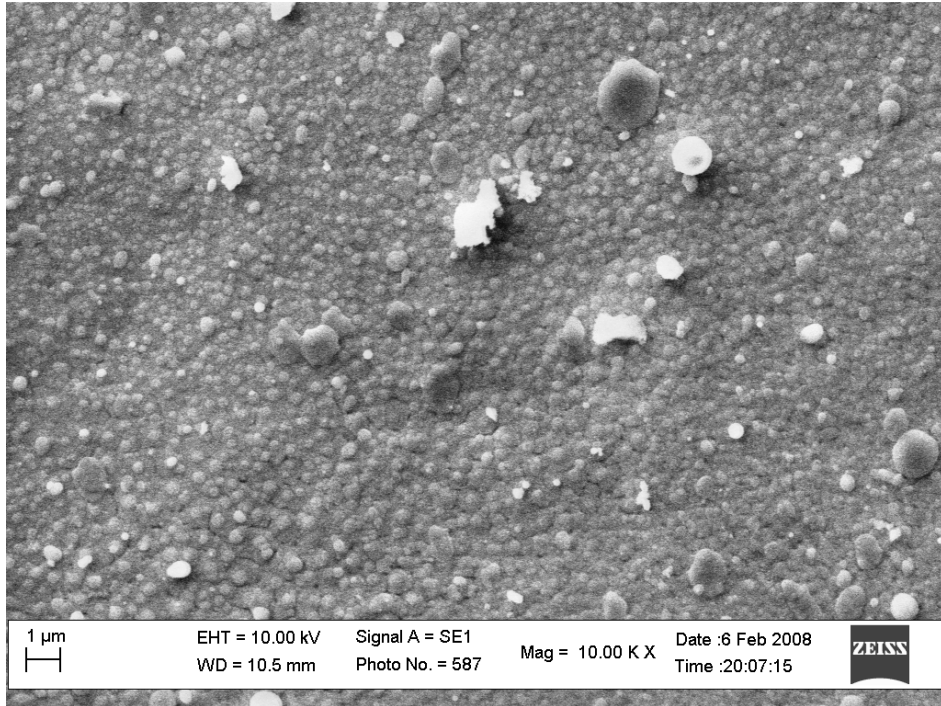
V.I.Krauz et al., Phys. Usp. (Advances in Physical Sciences), 53 (10) (2010)

Surface Morphology in the Discharge without Injection Al_2O_3 (SEM)



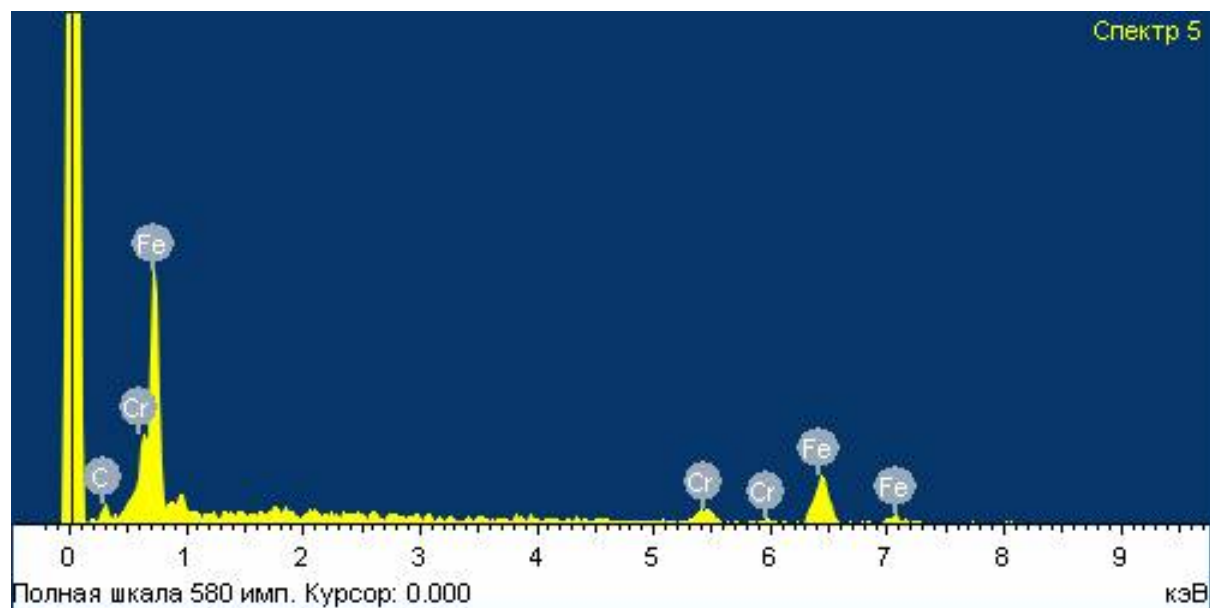
The surface has structure with the characteristic size $\sim 10 - 50$ microns and monotonous change of a relief. On scales of an order of micron a relief is homogeneous enough.

Surface Morphology in the Discharge with Injection Al_2O_3 (SEM)

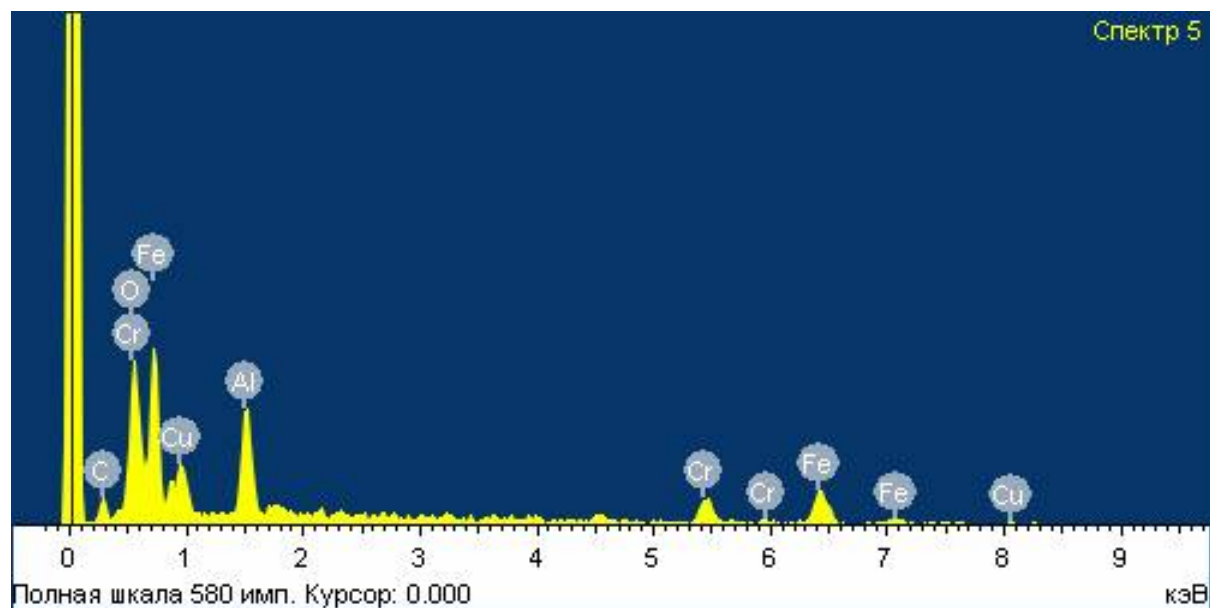


EDX

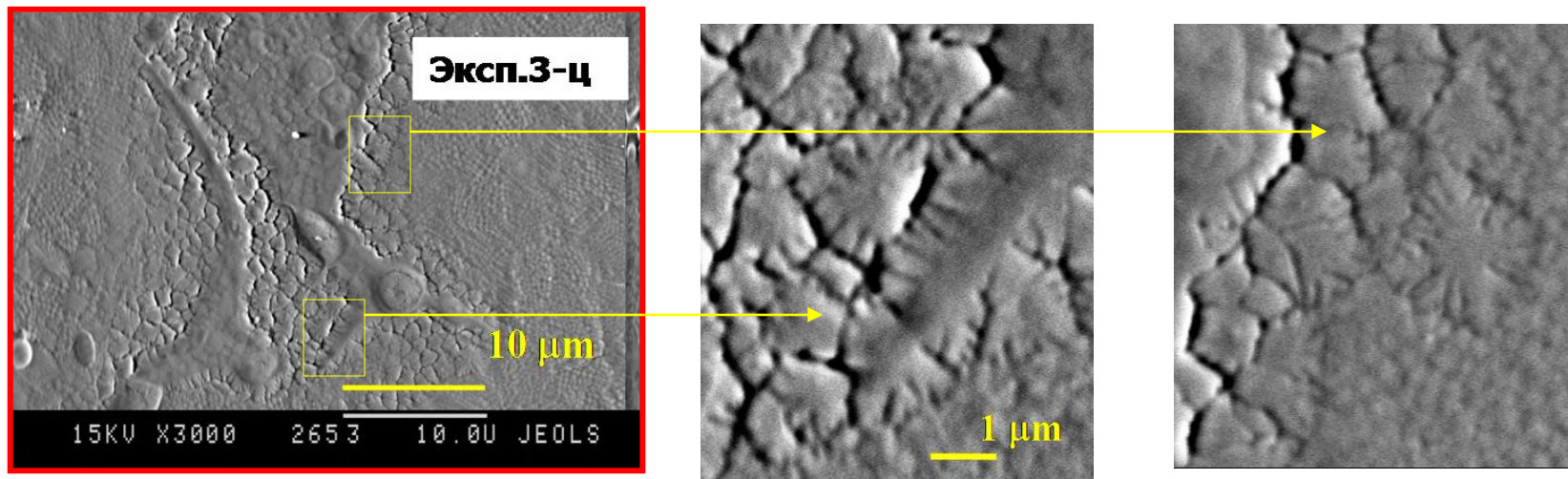
Without powder



With powder

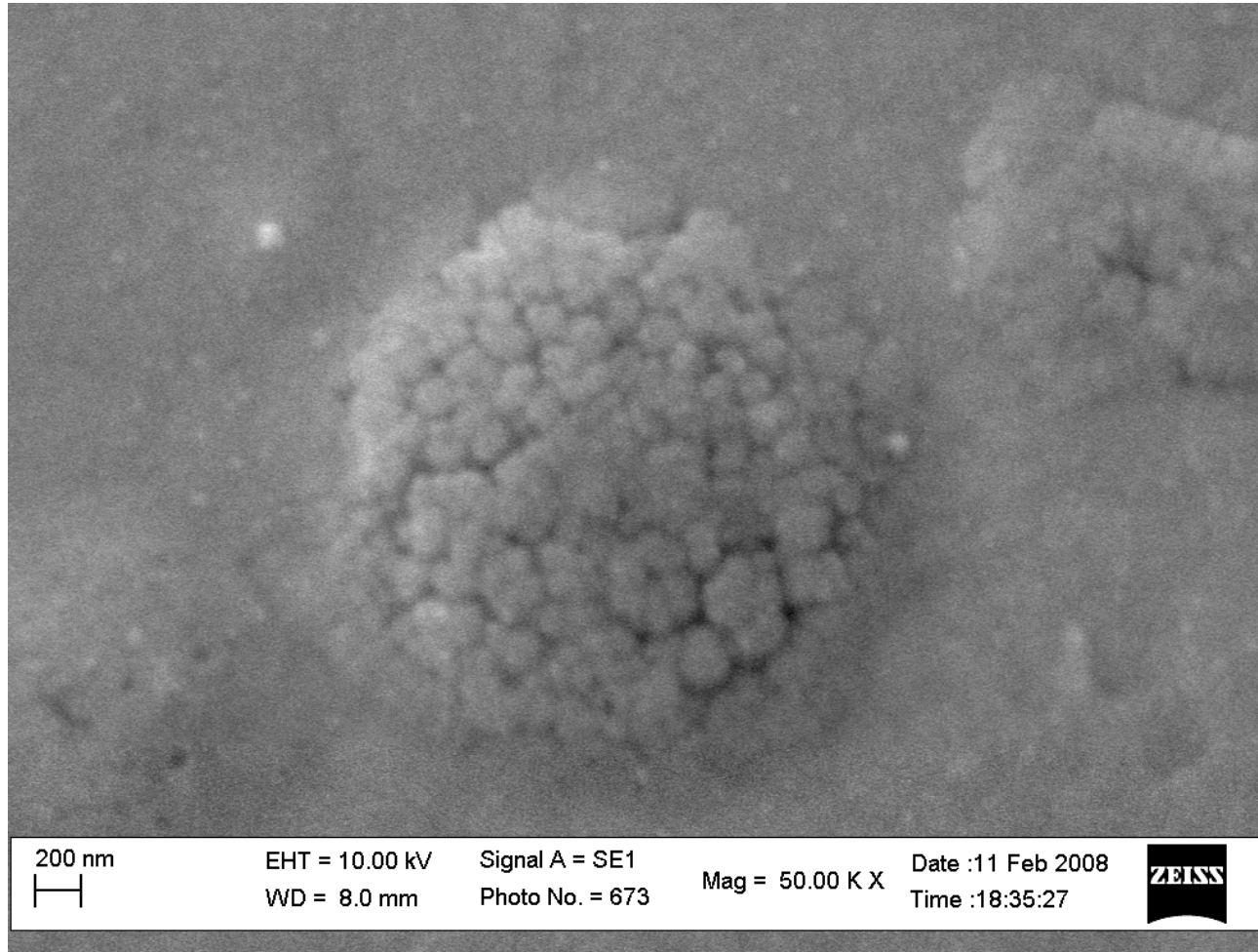


Surface Morphology at High Energy Input



“Snowflake” clusters

Fractal nano-cluster



The powder injected in plasma focus, deposits on the substrate as fractal particles or nano-clusters. Such structures have high developed surface that is the extremely important for various technological applications: medicine (pacemakers), catalysts, new power supplies, etc.

Conclusion

- **Filippov-type plasma focus originate the history actually from the very beginning of the Z-pinch studies (and Control Fusion in whole !)**
- **Despite similarity of the final pinch and radiation parameters in Filippov-type and Mather-type devices there are essential distinctions in initial, preparatory stages of the discharge, and, as a result, in mechanisms of generation of radiations**
- **Use of these special features for development of some new directions of researches is represented expedient. It concerns first of all the possibility to control the PCS shape, preheating of targets by radiation of PCS, etc.**
- **Plasma focus facility PF-3 operates at the discharge current up to 4 MA. It allows to consider it as a very promising source of SXR and perform many new interesting experiments in different branches of plasma physics.**

Acknowledgments

The author would like to thank

V.Myalton, A.Mokeev, V.Vinogradov, Yu.Vinogradova (*PF-3 team*)

V.Smirnov, V.Kojdan, L.Khimchenko, V.Lisitsa, M.Levashova,

V.Vichrev and many others...

(Kurchatov Institute)

K. Mitrofanov (*TRINITY*)

for their invaluable contribution to the PF-3 performance
and obtained results

We are grateful to **E.Khautiev** and **M.Karakin** who have made an essential contribution to the PF-3 operation, but, unfortunately have passed away, and of course, to

N.Filippov and **T.Filippova**

not only for PF-3-facility, but also for all PF direction created by them.